gear TECHNOLOGY™

MARCH/APRIL 2025

Steel Tariffs
Heat Treating
Differential Gears
Contract Manufacturing

TECHNICAL

The Role of In-Situ Techniques in Microstructure Optimization of Interstitially Alloyed Steels

Decarbonization of the Iron and Steel Sector: Challenges and Opportunities

Gear Technology is POWERED by The American Gear Manufacturers Association

geartechnology.com

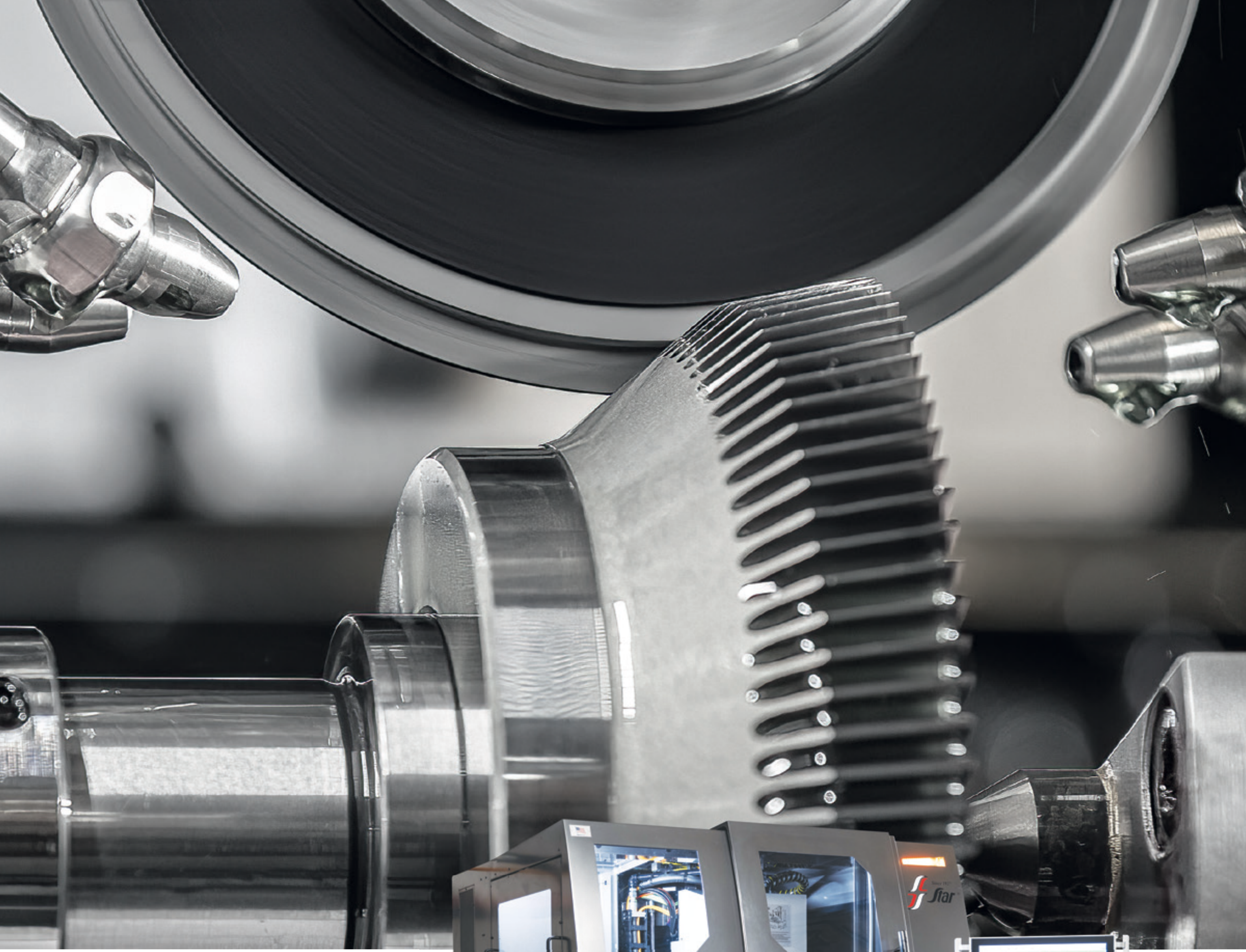


NXT

CONTENTS

gear TECHNOLOGY

MARCH/APRIL 2025

feature

22

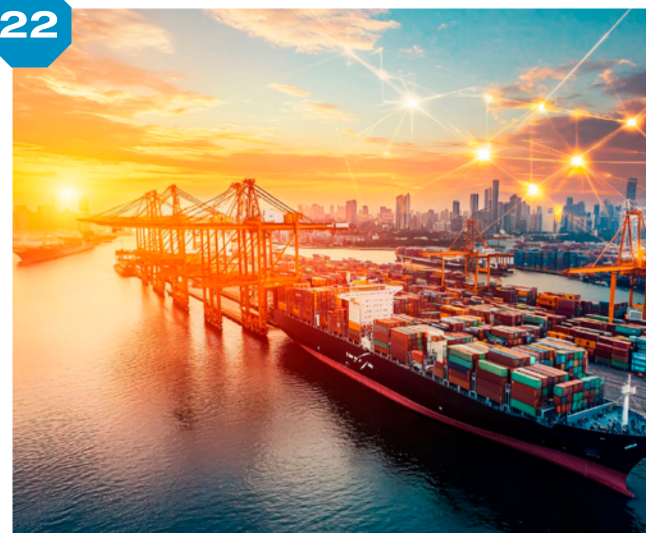

technical

34

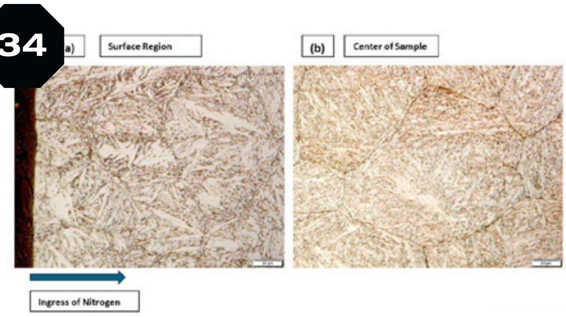

Stay Connected

gt Subscribe Online *geartechnology.com/subscribe.htm*

Join the Gear Technology Facebook group at *facebook.com/groups/geartechnology*

Connect with us on LinkedIn *linkedin.com/groups/3893880/*

Vol. 42. No.2 GEAR TECHNOLOGY. The Journal of Gear Manufacturing (ISSN 0743-6858) is published monthly, except in February, April, October and December by The American Gear Manufacturers Association, 1001 N Fairfax Street, Suite 500, Alexandria, VA 22314, (847) 437-6604. Periodical postage paid at Arlington Heights, IL, and at additional mailing office (USPS No. 749-290). The American Gear Manufacturers Association makes every effort to ensure that the processes described in GEAR TECHNOLOGY conform to sound engineering practice. Neither the authors nor the publisher can be held responsible for injuries sustained while following the procedures described. Postmaster: Send address changes to GEAR TECHNOLOGY. The Journal of Gear Manufacturing. 1001 N Fairfax Street, Suite 500, Alexandria, VA 22314.


DVS TECHNOLOGY AMERICA
Buderus SCHLEIFTECHNIK
ONE INSTEAD OF THREE
Grinding. Turning. Measuring. uFlex can do it!
Multi-function head with up to five tools
Hard machining for less setup time
22” ergonomic panel for easy operation
Compact design for maximum efficiency
Granite machine bed for precision.

gear TECHNOLOGY®

Vol. 42. No. 2

gear™ TECHNOLOGY

GT EXTRAS

The Tools Essential to Power Skiving

The rise of power skiving to a preeminent cylindrical gear cutting process has been one of the gear industry's most compelling success stories in recent decades. What began many years ago as a promising, but specialized, cutting process alternative for cylindrical gears with challenging interference contours is now exceeding performance and application expectations across the board.

geartechnology.com/the-tools-essential-to-power-skiving

Machine Tool Magic

Klingelnberg recently invited customers to its first Open House in Saline and the two-day event did not disappoint. Customers from major automotive, off-highway, construction and agriculture OEMs attended a morning of technical presentations before heading into the showroom to learn more about Klingelnberg's latest machine tool technology.

geartechnology.com/machine-tool-magic

Mandelbrot Meets Machine

Benoit B. Mandelbrot (1924–2010), the mathematician who coined the term "fractal," revolutionized the way we understand complexity in nature. His groundbreaking work introduced the concept of self-similar patterns—structures that repeat at varying scales—which appear in phenomena as diverse as coastlines, clouds, and market fluctuations.

geartechnology.com/mandelbrot-meets-machine

I NEED YOUR INPUT

Literally, I need your input—as in data.

If you haven't stopped by recently, you may not be aware that we've completely redesigned *geartechnology.com* (and *powertransmission.com*). We started from scratch and rebuilt the sites from the ground up to serve, you, the readers.

But in order to serve you best, I need you to do three things:

- [ ] **Subscribe/Renew.** By filling out the form to renew your FREE subscription to *Gear Technology*, you help us keep your data up to date. You also provide us with vital information that helps us continue to deliver the best possible technical content to meet your needs.

- [ ] **Visit the Buyer's Guide.** If you are in the market for any machines, tooling or services related to gear manufacturing, or if you need to find suppliers of gears, gear drives or gear manufacturing services, our online directory is the go-to resource. *(And if you are one of the aforementioned suppliers—and you're not listed—take a few minutes to fill out the fast and easy form at* geartechnology.com/get-listed.*)*

- [ ] **Explore the site and send feedback.** You can reach anyone on the AGMA Media team by visiting *geartechnology.com/contact-us*. Or you can send a message directly to me via *geartechnology.com/contact-randy-stott*.

We'd love to hear from you. But most of all, spending a few minutes to fill out these fast and easy forms helps us continue to make *Gear Technology* the gear industry's information resource.

Randy Stott

Publisher & Editor-in-Chief
Randy Stott, Vice President Media

KISSsoft

PRESENTS LOAD SPECTRUM CALCULATION

The *KISSsoft System Module* is a user-friendly tool also for load spectrum calculation designed for gearboxes. It incorporates nominal boundary conditions, variable forces on shafts, gear shifts, and hence changes in the power flow and operating mode variations. This complexity allows comprehensive calculations based on actual operating data, such as vehicle simulations or in situ measurements. This is particularly valuable for hybrid drive transmissions, continuously variable transmissions, and considering driving vs. coasting operation. For all bins in the load spectrum, the power losses are calculated, informing about the transmission efficiency. Each load case in the spectrum also serves as a nominal load for a single load calculation. Detailed reports for gears, bearings, and shafts clearly present key data, while the software supports easy export of load data for in-depth component analysis. Its intuitive interface ensures fast, accurate, and reliable calculations while saving engineer's time.

kisssoft.com

L.S. Starrett

INTRODUCES AUTOMATED INSPECTION TECHNOLOGIES AT MANUFACTURING TECHNOLOGY SERIES EAST

The L.S. Starrett Company will be featuring the automated inspection capabilities of its metrology and force measurement systems at Manufacturing Technology Series East (formally known as EASTEC) Booth #3244 at Eastern States Exposition in West Springfield, MA from May 13–15 this year.

Starrett optical and video-based measurement systems combine high-resolution images, powerful intuitive software and precision mechanical platforms to deliver superb accuracy and repeatable measurement results.

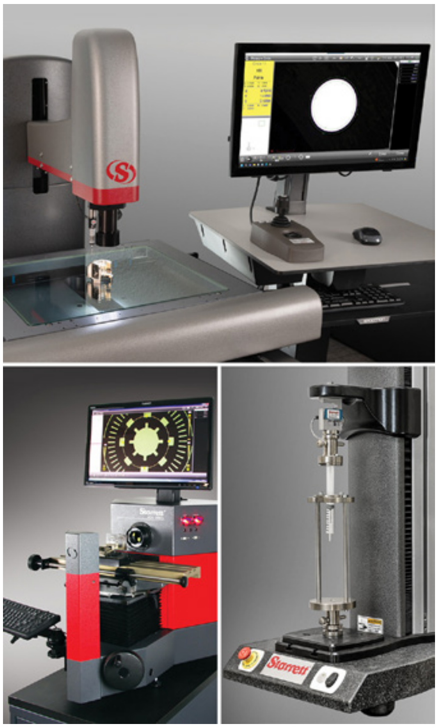

Starrett will demonstrate pattern recognition and automated inspection on several metrology systems at Manufacturing Technology Series East including:

- AVR400 CNC Vision System, features the largest benchtop platform to date from Starrett with stage travel that is twice the speed of previous Starrett AVR models. The stage travel is 15.8 in. x 11.8 in. x 7.9 in. (400 mm x 300 mm x 200 mm) in the X-Y-Z axes with a speed of up to 120 mm/sec.
- KMR-MX 200 Manual Vision System, a unique platform that fills the gap for companies that want the speed and accuracy of a video-based platform but do not need or want a PC-based system.
- HDV Horizontal Digital Video Comparator, which combines the best features of Vision and Optical Comparator technology.
- HD400 Horizontal Dual Lens Optical Comparator offering a two-lens mount, enabling instant switching between two magnification lenses or video camera adapter.

Starrett will also showcase its Force Testing Systems, highlighting the flexible architecture that enables the range of Starrett force and material testing software programs to be compatible with its different test frames. At Manufacturing Technology Series East, Starrett will demonstrate its FMS Series test frame measuring the force to draw fluid in and out of a syringe. This application uses Starrett *L2Plus* software to capture peak and average load data. FMS Force Testing Systems provide cost-effective, higher-volume production, and more consistent results over manual testing methods solutions for determining load, distance and break applications.

starrettmetrology.com

Ceratizit

RELEASES UP2DATE SOLUTIONS FOR INTRICATE MILLING AND MICROMACHINING

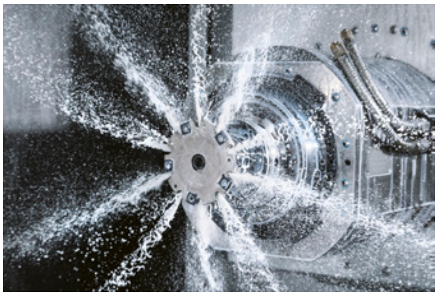

Ceratizit's UP2DATE catalog is now available, showcasing the latest product developments and advancements for the cutting tool industry. Designed to help customers optimize machining performance, extend tool life, and maximize production efficiency, this edition features tooling solutions tailored to meet intricate milling and micromachining operations. Included in the spring 2025 UP2DATE edition are the MaxiMill—Slot-SNHX milling cutter, the MaxiMill—Tangent milling cutter, and the WTX—Micropilot microdrill.

"Customers come to us for more effective and productive cutting tools which we deliver with support and technical expertise," says Troy Wilt, managing director of Ceratizit USA. "Applying our technical expertise in the field often leads to new and better solutions that work across multiple industry sectors."

Groove Milling Made Easy

The MaxiMill—Slot-SNHX is a robust side and face milling cutter system that is engineered for exceptional performance across a range of materials, including steel, cast iron, and aluminum. The innovative tool is designed to deliver soft cuts while effectively avoiding interfering contours, making it an ideal solution for diverse milling applications.

The MaxiMill—Slot-SNHX features trouble-free contours on the face side and sufficient axial freedom of movement that ensure smooth machining—even in hard-to-reach areas. Thanks to precision-ground indexable inserts, machinists can expect a flat groove base that ensures perfect surfaces from the very first cut. The system is also equipped with an internal coolant supply up to a diameter of 200 mm, which minimizes chip jamming and further boosts efficiency.

The MaxiMill—Slot-SNHX is available in three models to offer the most universal connection on the market. These slip-on milling cutters offer diameter ranges from 80 mm to 200 mm each of which include internal coolant supply, and multiple sized cutting widths. The screw-in milling cutter also provides an internal coolant supply on diameters of 50 mm, 63 mm, and 80 mm and cutting widths of 6 mm and 8 mm. The milling cutter with cylindrical shank and internal coolant supply is available to customers in diameters of 50 mm, 63 mm, 80 mm and 100 mm as well as cutting widths of 6 mm and 8 mm.

Better Reach and Pace

The MaxiMill—Tangent is Ceratizit's new tangential indexable milling cutter designed for machining hard-to-reach steel or cast-iron components. Engineered to deliver stable and soft-cutting machine, it provides a uniform chamfer profile over the entire length of the cutting edge for maximum stability within a single system.

The MaxiMill—Tangent has indexable inserts optimized for machining ISO P and ISO K materials. Moreover, it features a maximum infeed depth of 8 mm for the -09 insert, while the larger model goes even further to 12 mm. The MaxiMill—Tangent includes universal -M50 and -F50 chip breakers, offering enhanced cutting-edge stability due to a reduced radial clearance angle.

Furthermore, there is an integrated face-cutting edge, which offers machining benefits, including uniform material removal that results in a smoother component surface. In addition, the cutting forces are distributed more evenly and reduce the load on both the tool and the machine.

The MaxiMill—Tangent is available in three mounting styles: shell mill, screw-in cutter, and straight shank. Cutter diameters range from 25 mm to 125 mm. The large and stable contact surfaces in the integrated carrier inserts provide additional stability and reliability. Plus, compared to radial systems, tangential clamping provides extra space for significantly more indexable inserts on the milling cutter body, thus guaranteeing maximum cutting-edge density and efficiency. Inserts can be rotated,

turned, and replaced quickly and easily to prevent any drop-offs in efficiency during tool changes.

A Complete Microdrill System

The WTX—Micropilot is an innovative microdrill used for spot drilling small components with intricate geometries. Working in tandem with Ceratizit's WTX—Micro, the pilot drill is small in stature and delivers big performance with exceptional accuracy and time-savings for micro-sized components.

The risk of micro-sized components becoming scrap is high. Several things can go wrong: drills run off, drill holes get crooked, tools break, and the workpiece itself can become damaged. With a special drill point angle of 160 degrees, the WTX—Micropilot guarantees maximum positioning accuracy and prevents wandering while drilling to achieve extreme precision within a single run. Since it is designed to co-drill with the WTX—Micro, the usual mirroring required for drilling inclined and curved surfaces with an inclination up to 50 is no longer necessary, saving time and tool changes.

Additionally, the WTX—Micropilot is coated in Ceratizit's Dragonskin for optimum chip clearance and extended tool life. It also has spiral internal cooling channels to ensure maximum flow of cooling lubricant for improved surface finish.

cuttingtools.ceratizit.com/us/en/tool-solutions/uptodate.html

Grob Systems

WILL DEMONSTRATE POWER SKIVING CAPABILITIES AT MANUFACTURING TECHNOLOGY SERIES EAST

Grob Systems, Inc. will demonstrate power skiving capabilities as well as innovative fir tree mill finishing on its highly productive Grob G550T 5-axis mill-turn universal machining center at Manufacturing Technology Series East (formally known as Eastec) Booth #1720 at Eastern States Exposition in West Springfield, MA from May 13–15 this year. Attendees can see how Grob meets and exceeds precision manufacturing demands and Grob personnel will be on-hand to answer specific customer application questions.

The Grob G550T offers maximum stability and excellent maintainability and provides the greatest possible positioning flexibility due to the axes large swivel range (230° in the A'-axis and 360° in the B'-axes). A horizontal spindle position permits the longest possible Z-travel path and optimum chip fall. The G550T features a unique arrangement of the three linear axes that minimizes the distance between the guides and the machining point (TCP), providing stability in part production. A tunnel concept permits the largest possible component (even in the case of with extremely long tools) to be swiveled and machined within the work area without collision. The three linear and two rotary axes allow 5-sided machining, 5-axis simultaneous interpolation, as well as Grob Traori-turning for precise cutting control. Grob machining centers are made in the U.S.A. at the Grob Systems full production facility in Ohio which has recently been expanded to 500,000 sq. ft. and can include advanced automation solutions for dramatically increased productivity.

grobgroup.com/en

Mazak

HIGHLIGHTS EZ SERIES AT WMTS IN CANADA

The Mazak Ez Series comes to Canada for the Western Manufacturing Technology Show (WMTS) in Edmonton. In booth #1205, Mazak will feature its QT-Ez 12MSY Horizontal Turning Center with multitasking capability and the VC-Ez 20 Vertical Machining Center, both from the Kentucky-built series of machines that puts Mazak quality and reliability within reach for virtually any shop with productive, space-saving efficiency at an affordable price.

For multitasking part processing, the QT-Ez 12MSY accommodates rotating tools and features two turning spindles along with Y-axis functionality for efficient single-setup Done in One processing of a wide range of parts. While the machine comes standard with a 12-in. chuck, Mazak offers smaller 8-in. and 10-in. options.

Like all QT-Ez Series machines, the QT-Ez 12MSY is equipped with integral motor headstocks, Hybrid MX linear roller guideways and pre-tensioned ball screws supported at both ends for reliable, thermally stable and precise machine axis movement. A new bed casting design provides outstanding rigidity, as well as streamlined chip flow to help eliminate chip accumulation. For ease of integration, the machine incorporates a 200–230-volt power supply system.

Along with optional spindles, chuck sizes and tailstocks, the QT-Ez Series is available with a complete range of additional cost-effective and popular options. These include Mazak's Automatic Tool Eye, chip conveyor, auto door, auto parts catcher and high-pressure coolant systems, all of which make it easy for shops to further improve productivity.

For vertical machining, Mazak's VC-Ez 20's rugged 40-taper spindle and space-saving design offer unprecedented performance and affordability with a full range of spindle, auto tool changer and chip/coolant management options. The cost-effective, highly configurable machine meets many production facility needs with a compact, space-saving design.

Enhanced operator ergonomics and a generous work area ease the loading and unloading of workpieces and tools, while an extremely fast rapid traverse rate of 1,654 ipm (42 m/min) in the X, Y and Z axes enables higher throughput. A 25 hp (18.64 kW) 12,000 rpm (standard) or versatile 29.5 hp (22 kW) 15,000 rpm (optional) spindle offers 81.13 ft-lb (110 Nm) of torque for additional production versatility.

All VC-Ez Series machines sport C-frame designs with X and Y axis motion via moving the table and saddle. For rigidity and repeatable part precision, guideway systems use Mazak's Hybrid MX linear roller guide systems, and dual lagged pre-tensioned ball screws ensure precise axis movement. For increased maintenance free operation, the auger-type chip removal systems provide an economical solution, or for increased chip volume the addition of an affordable hinge-type chip conveyor ships affixed to the machine to eliminate the cost of a second shipping pallet.

mazak.com

TCI Precision Metals

INTRODUCES CUSTOM–CUT, READY–TO–SHIP BLANKS

TCI Precision Metals has introduced custom-cut, ready-to-ship blanks. Customers can now order custom-sized, pre-machined materials that ship fast and arrive ready to go directly from receiving to finish machining.

"Ready-to-ship blanks, available online from TCI Precision Metals, are pre-configured in hundreds of dimension/alloy combinations. Each blank arrives at the customer flat, square, parallel, and ±.002 in. of stated dimensions. When customer dimensional requirements fall between standard available sizes, they can order the custom-cut option and get exactly what they need. This is important, especially when customers want to go directly from receiving to machining without any further prep." said Ben Belzer, president and CEO of TCI Precision Metals.

Ready-to-ship blanks help shops shorten setup time, reduce scrap, and increase overall throughput by up to 25 percent by eliminating material prep. Blanks arrive machine-ready for production and are ideal for short-run and production machining, tooling, and prototype applications.

Precision blanks eliminate the need for in-house sawing, grinding, flattening, squaring operations, and outside processing. Blanks are consistent, part-to-part, which reduces setup time. In the case of flat blanks, the production process alleviates residual stress in the material, which results in reduced part movement during finish machining. Each blank is deburred, cleaned, and individually packaged to avoid damage during shipping.

tciprecision.com

Star SU

OFFERS NEW LOUIS BÉLET DRILL LINE DEDICATED TO STAINLESS STEEL

Star SU, Star Cutter Company's marketing, sales and service affiliate, announces the availability of a new line of expert internal coolant drills from Louis Bélet, designed specifically for stainless steels. This drill line is suited for application in all fields where stainless steel is used, such as watchmaking, medical, aerospace, automotive, etc.

Machining of stainless grades, such as martensitic and austenitic, is often slow and prone to errors. To address these challenges, one of the drills in the new range (REF .376-10) achieves depths of up to 10xd and at rates that are 3x to 4x faster than previous drills. It also eliminates the need for pecking, resulting in smoother, more productive operations. Further, to eliminate the need for a centering or deburring device, a second drill (REF .336H) can be used, with or without a chamfer, to produce a pilot hole.

These drills are designed with a compression chamber that minimizes coolant pressure loss, improving efficiency and accuracy with the drills able to hold concentricity of <0.003 mm at the drill tip. Additionally, an increased surface area of the lube holes and their specific shape enable these drills to achieve 3x the throughput compared to previous generations.

To tackle complex stainless steels and even superalloys like CoCr (Phynox), Louis Bélet developed a micrograin carbide specifically for stainless steel applications. The TiSi (titanium-silicon) coating reduces friction, decreases heat buildup, and prevents burr formation, ensuring longer tool life. The unique cutting-edge preparation also ensures optimal coating adhesion and durability for longer tool life.

Star SU is the exclusive representative of Louis Bélet SA (Switzerland) precision cutting tools in North America.

star-su.com/partners-brands/louis-belet/

KUKA

ADDS KR IONTEC ULTRA TO ROBOTIC PORTFOLIO

The new KR Iontec ultra completes KUKA's portfolio in the payload range of 80 to 120 kg. With a reach of 2,300 to 2,700 mm, this compact and powerful robot offers maximum efficiency and flexibility in the modern production environment—for example in handling or spot welding with lightweight welding guns.

Thanks to its compact design, the KR Iontec ultra can easily find its way into even the tightest of spaces: customers can use the slim robot to create narrow automation cells. As a result, the space saved leads to lower costs. In addition to the small footprint, the robot has very good performance, which helps to minimize cycle times.

The KR Iontec ultra fits seamlessly into the KR Iontec family, which has impressively low maintenance requirements: an oil change is only necessary every 20,000 operating hours and the central hand concept does not require belts. The robot has a streamlined build with fewer breakable small parts.

The all-rounder demonstrates its strengths in handling—especially in the battery area—and in spot welding with lightweight welding guns (lightweight spot welding). With its payload of up to 120 kg, the robot can move heavy battery cells and modules for use in electromobility. The slim robot also fits perfectly into compact welding cells—a feature that is highly sought after by suppliers to the automotive industry, for example.

In the KUKA portfolio, the KR Iontec ultra has the advantages of both the KR Iontec and KR Quantec product families. With a smaller footprint than the KR Quantec and high performance at the same time, it is a cost-effective option for entry-level automation. "The KR IONTEC ultra can be quickly and intuitively integrated into existing production environments," says Michael Laub, platform product manager medium payload and palletizing robots at KUKA.

As the robot can be implemented with the KUKA.PLC mxAutomation interface, it can be programmed and operated by the user in a familiar control environment. This means that the compact, powerful and cost-efficient robot can quickly make its contribution to production in various handling applications and in spot welding with lightweight welding guns. The KR IONTEC ultra with a payload capacity of 120 kg and a reach of 2,700 mm is available to order now, with three further model variants to follow this summer.

kuka.com

Machine and Tool Concepts for Contract Manufacturing

Liebherr solutions enhance flexibility, accuracy, and efficiency at SPN Schwaben Präzision

Thomas Weber, Head of Marketing, Liebherr-Verzahntechnik GmbH

Wide range of parts and short setup times for gear shaping with the LS 180 E.

The Swabian transmission and drive solutions manufacturer SPN Schwaben Präzision Fritz Hopf GmbH manufactures gearboxes, gears, and drive systems according to individual customer requirements. (Swabia is a region in southwestern Germany known for its engineering and manufacturing excellence.) SPN relies on various machine and tool technology from Liebherr-Verzahntechnik GmbH.

SPN was founded over 100 years ago in Glashütte, Saxony as a workshop for contract gear manufacturing. After the war, the company moved its headquarters to the Swabian town of Nördlingen and initially manufactured precision gears for watches. Today, around 300 employees there develop and manufacture gearboxes, gearing components, drive systems and components for drive technology and mechatronics. "We manufacture customer-specific drive components and gearboxes with the highest precision," says Stefan Ohmüller, head of production technology at SPN. The company is continuously investing in the expansion of its production capacities and over time has developed into a true one-stop shop for gears. The wide variety of parts is now being manufactured, among other things, on seven machines from Liebherr-Verzahntechnik GmbH. The company also purchases tools and clamping devices from Kempten.

Advancing Gear Shaping Technology for Increased Efficiency

For many years, SPN has been using Liebherr gear shaping machines for workpieces with diameters of up to 300 mm. To absorb production peaks and increase capacities, in 2018 the two existing machines for gear shaping were supplemented by an LS 180 E, which offers a range of benefits: its shaping head is equipped with an electronic helical guide that facilitates frequent workpiece changes. The helix angle can be easily and continuously adjusted via the clear user interface of the *LHGearTec*. This allows it to machine a wider range of parts and also reduces setup times. Automatic loading allows several machines to be operated at the same time. "Due to our different quantities, we still need machines that can be operated manually, but at the same time place great value on multi-machine operation. Automation helps us here," explains Ohmüller.

Gear Grinding Machines for High Profile Accuracy

SPN relies on the LCS 150 generating and profile grinding machine from Liebherr-Verzahntechnik GmbH for the high-quality requirements associated with flank grinding. Among other things, this offers numerous advantages for job shops: both CBN and corundum tools can be used, an integrated device quick-change system and automatic clamping fixtures reduce setup times considerably, and automatic loading by a ringloader with two stations supports the multi-machine concept. The LCS 150 can machine even the smallest drive pinion with a module of 0.4 with the highest profile accuracy. SPN was so satisfied with the performance that they purchased another gear-grinding machine, the LGG 280, in 2022.

Maximum profile accuracy when grinding with the LGG 280.

For Related Articles Search
manufacturing
at geartechnology.com

Machine acceptance of the LC 500 DC in Kempten: Head of Production Technology at SPN Stefan Ohmüller and Liebherr Area Sales Manager Thomas Butzke are satisfied.

Gear Hobbing Machine with Integrated Chamfering Device

Due to increased order volume for a large agricultural machinery manufacturer, an LC 500 DC was added to SPN's machinery in April 2024. The decisive factor in their decision to purchase it was the integrated machining unit, which combines two chamfering technologies in one machine—a special feature of the new generation of machines. In addition to the fast, economical ChamferCut process, FlexChamfering—chamfering with common end mills—is particularly attractive for SPN, as it is suitable for small batch sizes. "As a specialist in customer-specific solutions, we often have smaller batch sizes and a large variety of parts, as we have to react very flexibly to customer requirements. Now we can produce defined chamfers with low tool costs, especially in small quantities," says Ohmüller. The flexible LC 500 DC enables a wide range of gears up to a diameter of 500 mm to be manufactured with cleanly reproducible results.

Everything from a Single Source for Smooth Processes

SPN uses Liebherr tools on all three shaping machines and takes advantage of Liebherr-Verzahntechnik's convenient pick-up service to have them sharpened regularly. SPN can keep an eye on the wear behavior of the shaper cutters thanks to the supplied simulation. "This means that we always know which root diameter the tool is currently making and can adjust the corresponding machine settings," explains Ohmüller. On the gear grinding machine, the flexible SECLA segment clamping arbor ensures short setup times. "Machines, tools and clamping devices from a single source provide us with a high level of production reliability," enthuses Ohmüller.

Ideally Suited for Contract Manufacturing

Overall, SPN was able to significantly reduce setup times on all Liebherr machines thanks to the ringloader concept and the quick-change interfaces, thus achieving a multi-machine quota increase of around 30 percent. The easy operation via the intuitive interface of the *LHGearTec* and the flexible correction options with the electronic helical guide during gear shaping are major advantages. "This is very important for us, especially concerning the customers' drawing specifications or the material behavior," emphasizes Ohmüller.

SPN also relies on proven Liebherr technology for automation. For example, the PHS 800 Allround pallet handling system was also used to interlink two machining centers in the production hall constructed in 2023, because it has a modular design, offers individual adjustment options and, above all, can be expanded if required. As a result, Ohmüller's summary is positive: "We have always done well with Liebherr, especially in terms of proximity, reliability and partnership. The LC 500 DC was certainly not our last Liebherr machine!"

liebherr.com

The Digital Ecosystem with Ipsen

IIoT, AI and automation integration leads to enhanced heat treat capabilities

Matthew Jaster, Senior Editor

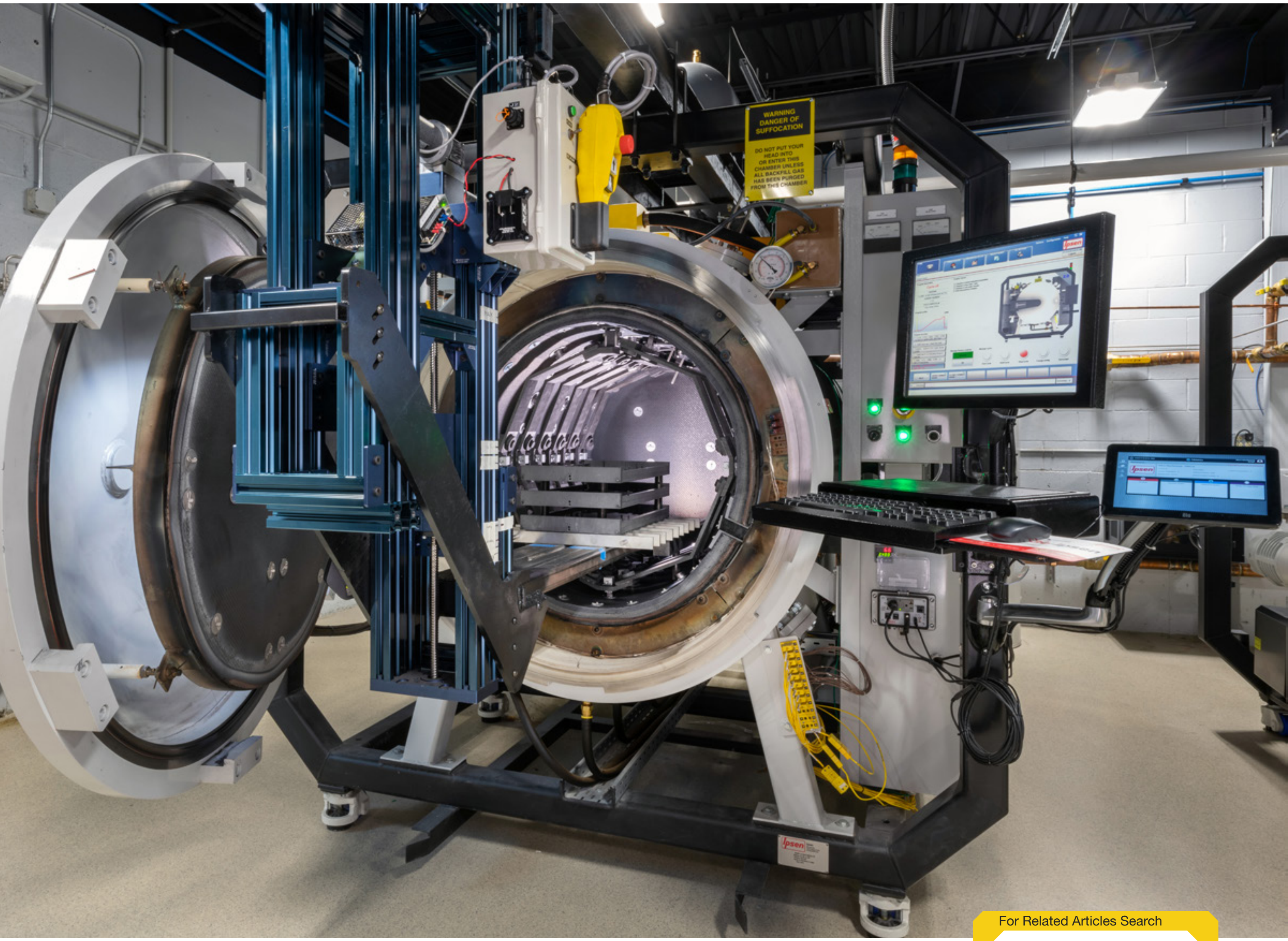

For Related Articles Search
IIoT
at geartechnology.com

By understanding customers' manufacturing and heat-treatment processes, Ipsen identifies pain points and develops IIoT and AI-driven solutions that improve operational efficiency.

"One of the biggest challenges in heat treating is unplanned furnace downtime, which leads to production delays and increased costs," said Aymeric Goldsteinas, Ipsen's vice president of digital technologies. "To address this, we are developing the next generation of PdMetrics, an AI-enhanced predictive maintenance system that uses sensors, machine learning, and anomaly detection to monitor furnace health in real-time. This allows customers to schedule maintenance before equipment failure occurs, minimizing disruptions and improving Overall Equipment Effectiveness (OEE)."

Additionally, digital transformation enhances the customer experience through self-service solutions. A key initiative in this journey at Ipsen is the online customer portal, Ipsen Connect, which serves as a one-stop hub for customers to manage equipment, service needs, and operational efficiency, all within an intuitive digital ecosystem.

"By integrating AI, IIoT, and automation, digital transformation helps customers minimize downtime, optimize spare parts management, enhance maintenance planning and improve workforce efficiency," Goldsteinas said.

Several areas within heat treating can significantly benefit from IIoT and AI-driven solutions:

- Predictive maintenance, such as Ipsen's *PdMetrics*, provides real-time health monitoring, notifying customers before failures occur allowing proactive maintenance scheduling.
- Spare parts management through tools like Ipsen Connect, which syncs with a CRM, allows customers to request quotes, reorder parts, and track shipping to ensure customers always have access to critical components.
- A centralized knowledge hub can utilize AI chatbots and advanced search engines to organize resources like troubleshooting guides, training videos, and best-practice articles. This approach allows users to quickly access relevant information, reducing reliance on external support and improving operational efficiency.

These solutions allow customers to maintain operational excellence with minimal disruptions.

In addition, digital transformation can drive significant improvements in resource efficiency for more sustainable manufacturing practices. Predictive maintenance for resource efficiency, for example, helps extend the lifespan of equipment by addressing issues before they lead to failures. This not only reduces unplanned downtime but also minimizes unnecessary material waste by optimizing the use of equipment and resources.

Energy optimization is captured using digital solutions such as real-time monitoring and adjustments which allow for more efficient energy use in heat-treatment processes, reducing overall energy consumption and lowering carbon footprints.

By providing insights into process improvements, digital solutions can reduce defects and rework, ultimately minimizing material waste. Optimizing production workflows also enhances overall productivity, which contributes to fewer resources being used per unit produced.

"As heat-treating facilities become more connected through IIoT and cloud-based solutions, cybersecurity and data protection will be critical for ensuring safe, uninterrupted operations. Key considerations include secure data management and remote access security," Goldsteinas said.

This includes using encryption and controlled access to prevent unauthorized access. As remote furnace monitoring and control become more prevalent, security protocols such as multi-factor authentication and VPNs are essential.

"Ensuring robust connectivity and cybersecurity measures will be vital for the future of smart manufacturing in heat treating," Goldsteinas added.

Smarter Technologies

Automation is revolutionizing heat treating by enhancing process accuracy, minimizing manual intervention, and increasing repeatability.

According to Goldsteinas, a smart furnace is defined by real-time data monitoring, AI-driven decision-making, and automated service management. Ipsen's next-generation digital solutions are shaping the future of smart furnaces with the following capabilities:

- IIoT-connected sensors: Measure temperature, pressure, and gas flow in real time.
- AI-powered predictive maintenance: Monitors equipment health status and detects potential failures.
- Automated parts and service management: Allows customers to track service history, request repairs, and order parts with a single click.
- Remote monitoring and control: Enables customers to access and adjust furnace parameters from any location.

The Future of Heat Treating

In general, smart furnaces offering AI/machine learning will provide better data, easier operation and the ability to stay ahead—and prevent—failures. This investment in data collection will provide long-term benefits if companies aren't scared away by initial costs and training expenses. As parts become more complex in the future, heat treaters will need additional resources to stay ahead of the competition.

Goldsteinas noted several areas where smart furnaces will continue to evolve from an IIoT and digital manufacturing perspective.

"Self-optimizing AI-driven operations is one," Goldsteinas said. "AI will automatically adjust heat-treatment cycles, optimizing energy use and part quality. Another is digital twin technology where virtual furnace models will simulate heat-treatment scenarios, allowing customers to test process adjustments before implementation."

Two more focal points in heat treating will be using the blockchain for traceability and AI for advanced troubleshooting.

"Heat-treated parts will have tamper-proof digital records, ensuring full process transparency and compliance," Goldsteinas said. "Using augmented reality (AR) for remote diagnostics will also reduce the need for on-site service interventions."

Ipsen is committed to continuously developing solutions that will make heat treating more autonomous, efficient, and sustainable now and in the future.

ipsenusa.com

Farewell to an Idea

The impact of steel tariffs on the gear industry

Aaron Fagan, Senior Editor

"Farewell to an idea," wrote Wallace Stevens in the poem *The Auroras of Autumn* (1947), exploring themes of change, impermanence, and the tension between imagination and reality. The phrase reflects Stevens' meditation on the fading of belief systems and the transience of human constructs. It's part of the broader contemplation in *The Auroras of Autumn* on the cyclical nature of life and the inevitability of endings.

Trade policy faces the end of stable, predictable global commerce—competing ideas are in a tug of war, and the tension between imagined futures and local reality is taut. Section 232 of the Trade Expansion Act of 1962 empowers the U.S. president to impose tariffs on imports deemed a national security threat. In 2018, it was used to justify tariffs on steel and aluminum, disrupting supply chains and prompting retaliatory measures from trading partners. At the time, manufacturers were allowed to apply for tariff exemptions through the Section 232 exclusion process if the materials were unavailable domestically or did not meet performance standards.

On March 11, 2025, the U.S. Department of Commerce announced it would terminate the Section 232 exclusion process, effective March 12, 2025. This limits manufacturers' ability to seek relief from higher material costs, particularly for specialized alloys used in gear manufacturing. Without the ability to apply for exclusions, manufacturers who rely on these materials now face even steeper price increases.

As of March 12, 2025, U.S. Customs and Border Protection (CBP) began enforcing Section 232 tariffs on foreign steel and aluminum, reigniting trade tensions with key global competitors and close allies. This action, part of broader measures to protect and revitalize the U.S. domestic steel and aluminum industries, places a 25 percent tariff on imports of these materials.

While domestic steel producers have welcomed the move, hoping it strengthens national production, its downstream effects on automotive, aerospace, and industrial manufacturing—including the gear manufacturing sector—threaten to erode market position and exacerbate supply chain challenges that many industries are already grappling with.

The Ripple Effect on Gear Manufacturing

Gear manufacturers rely on high-chromium and high-nickel steels that are crucial for producing high-performance gears in demanding applications such as aerospace, defense, and heavy machinery. However, many of these materials are not made in sufficient quantities or with the required quality within the United States.

In the aerospace industry, for example, gears used in jet engines, turbines, and landing gear systems are often made from Inconel, Hastelloy, and maraging steels—materials known for their strength, oxidation resistance, and ability to withstand extreme temperatures and stresses. In marine applications, offshore drilling rigs, naval vessels, and submarine gears require materials resistant to saltwater corrosion and high pressures, such as 316 stainless steel and Ni-Cr alloys. Similarly, in the oil and gas industry, high-nickel steels like Hastelloy C276 and Inconel are indispensable in drill rigs and pumps subjected to harsh chemicals and high heat.

The tariffs will have a domino effect on production timelines and manufacturers may be forced to absorb the higher costs, pass them onto customers, or face reduced sales share in domestic and international markets. This is especially concerning for manufacturers relying on specialized materials to meet stringent performance standards across automotive, power generation, and chemical processing industries.

Join AGMA/ABMA in Washington, D.C. to Shape Steel Trade Policy

On May 12–13, 2025, industry leaders from the gear and bearing sectors will gather in Washington, D.C., for the ABMA/AGMA DC Fly-In—a two-day event focused on engaging directly with federal agencies and lawmakers. This is a key opportunity for manufacturers to have a seat at the table and help shape the policies that impact the power transmission manufacturing sector.

Sessions will run from 8:00 a.m.–5:00 p.m. each day, with meetings and discussions involving representatives from the U.S. Trade Representative, U.S. Customs and Border Protection, Homeland Security Investigations, the Department of Commerce, and the National Security Council. Capitol Hill meetings will allow attendees to engage with senators and congressional representatives, helping lawmakers understand the strategic importance of domestic manufacturing and the challenges posed by tariffs and rising material costs.

Register through the American Bearing Manufacturers Association (ABMA).

americanbearings.org

agma.org

No Section 232 Exclusions

Under previous tariff cycles, manufacturers could apply for exclusions through the Section 232 process if domestic suppliers could not meet specific material needs. With the removal of the Section 232 exclusion process, manufacturers can no longer apply for new product exclusions, and pending applications will not be reviewed. Existing general approved exclusions (GAEs) have also been revoked. This shift removes a key avenue for relief, leaving gear manufacturers with limited options.

Exploring Alternative Strategies

Without the exclusion process, gear manufacturers must find ways to offset the economic impact:

- Reclassification: Some manufacturers may seek to reclassify materials under a lower tariff category, though this requires coordination with customs specialists.
- Foreign Trade Zones (FTZ): Operating within an FTZ may allow manufacturers to defer, reduce, or eliminate certain duties on imported steel. However, the administrative burden of managing an FTZ—complying with U.S. Customs and Border Protection (CBP) regulations, tracking inventory, and ensuring proper record-keeping—can be a barrier, especially for smaller manufacturers. While FTZs were previously used as a strategic workaround, it remains unclear whether their benefits will be as effective following the removal of Section 232 exclusions.

The Political and Economic Outlook

The broader economic and political consequences of the 2025 tariffs remain uncertain. While similar tariffs imposed in 2018 saw an uptick in domestic steel production, U.S. manufacturers also faced diminished profits and commercial edge in international markets. In the short term, the tariffs are contributing to inflationary pressures and uncertainty, adding complexity to the already strained global supply chains.

"While American businesses are incredibly resilient, we need time and adequate warning to implement such significant adjustments," said John Cross, CEO of ASI Drives. "The rapid succession of changes is difficult to manage, placing a disproportionate burden on small manufacturers. This forces us to spend valuable time on nonrevenue-generating tasks instead of focusing on growing our business."

Retaliatory tariffs from the European Union and Canada may deepen these disruptions, compounding the difficulties for manufacturers who rely on global trade for cost-effective materials. At the same time, the market for steel and aluminum remains volatile, with rising prices reflecting the ongoing uncertainty about the impact of these tariffs.

Protecting Presence in a Shifting Market

While the 2025 tariffs may provide a boost to domestic steel production in the short term, they pose a challenge for U.S. gear manufacturers. Manufacturers must act swiftly to secure revised sourcing strategies, reclassify materials, or establish operations within FTZs.

Furthermore, industry associations such as the American Gear Manufacturers Association (AGMA) and the American Bearing Manufacturers Association (ABMA) will play a key role in advocating for relief and pushing for policy adjustments that protect manufacturers' long-term competitiveness.

"ABMA and AGMA know that the current environment poses new challenges and opportunities to the industry, and we want to hear from our members on how they are affected by tariff and regulatory changes," said Jenny Blackford, president of ABMA and chief operating officer of AGMA. "In May, we look forward to bringing the story of our industry—its impact on the economy, national security, and the workforce—to the leaders in Washington so that they can be better informed on what our industry needs to continue to grow in the United States."

A New Process for Differential Gear Manufacturing

Enhancing strength, efficiency and quiet performance for electric vehicles

Prof. Dr. Hermann J. Stadtfeld, Vice President Bevel Gear Technology and R&D, Gleason Corporation

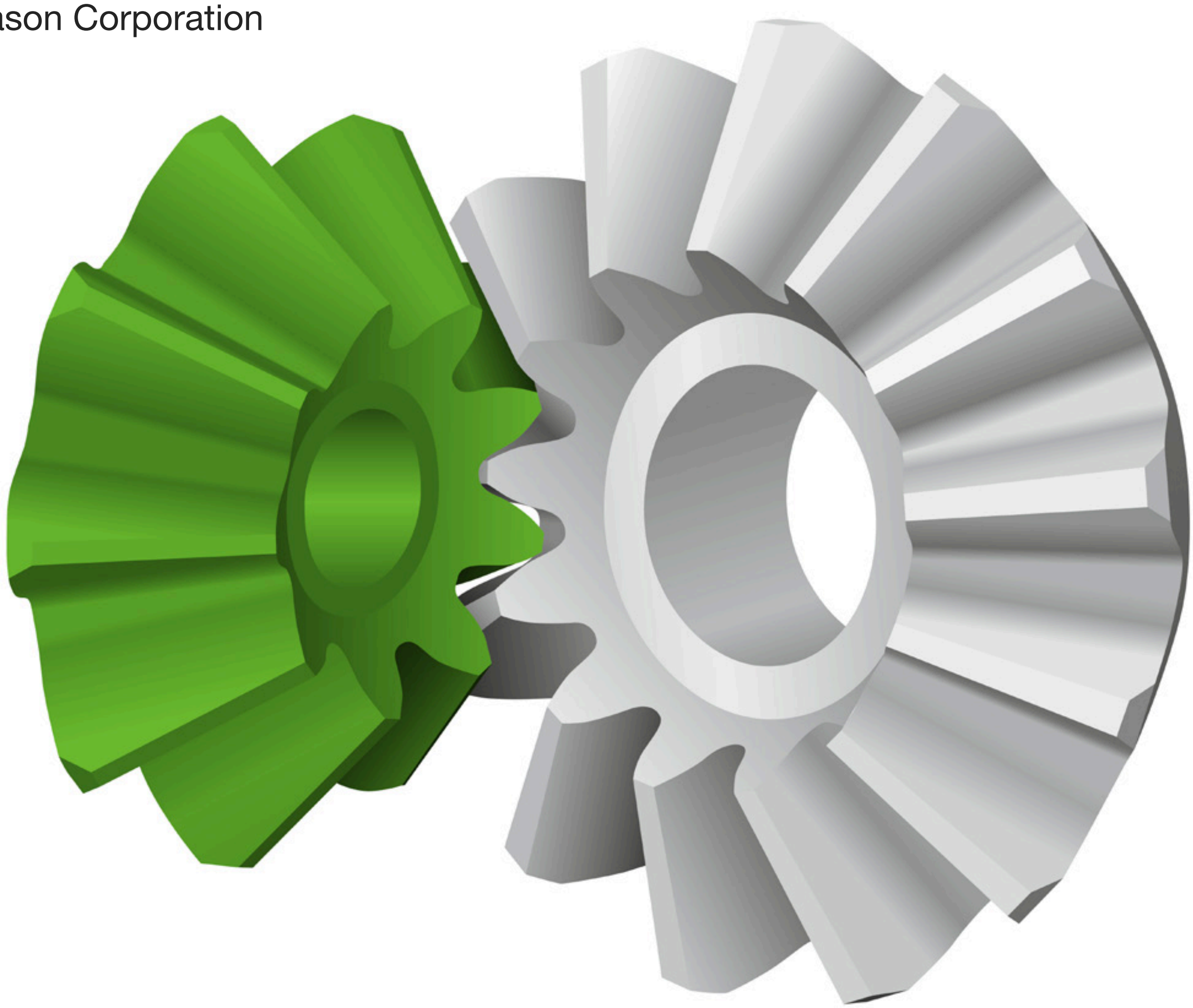

The manufacturing of differential gears went away from the Revacycle broaching process to forging more than 30 years ago. Today, where electric vehicles create a peak torque which are a multiple higher than in vehicles with internal combustion engines, the strength and the Noise Vibration Harshness (NVH) advantages of cut differential gears are revisited. The newly developed Coniflex Pro straight bevel gears combine several new features which make them stronger and quieter than past straight bevel gears and far superior to the forged version. The basic geometry of Coniflex Pro was developed especially for modern Phoenix free-form CNC machines and takes advantage of the "unlimited" geometric freedoms and the possibility of higher order, nonlinear kinematics. First field applications have proven that Coniflex Pro differentials have 30 percent lower root bending stress and 40 percent lower surface stress as forged differential gears. Many electric all-wheel drive vehicle applications with a front axle disconnect feature create high relative motions in the differential of the disconnected axle, which makes the transmission very noisy. Coniflex Pro gears have the lowest transmission error of any ever-produced straight bevel gear. While transmission errors of 50 microradians (µrad) or less are typical for Coniflex Pro, conventionally cut or forged straight bevel gears show between 300 and 2,000 µrad. Coniflex Pro differentials are therefore exceptionally quiet, even in case of high relative motions in disconnect axles.

Generating on the Pitch Cone

All the older straight bevel gears are generated by rolling on the root cone, rather than on the pitch cone. Figure 1 shows to the left the traditional orientation between the generating plane and the pitch cone of a gear. This orientation violates the kinematic coupling condition between gear, generating plane and pinion. Both mating Coniflex Pro members roll with their pitch cones on the common generating gear plane as shown to the right in Figure 1. This was not possible in the past because the tip circle of the cutting tool had to be adjusted to the root angle of the tapered depth teeth of the gears and due to the mechanical restrictions of older machines, the generating gear rotation was automatically orthogonal to the root line of the cut gear. Thus, the gears were generated on the root cone rather than on the pitch cone.

Free-form Phoenix machines do not have the traditional mechanical restrictions. Therefore, the choice of adjusting the cutter tip circle tangential to the root line of the cut pinion and gear and yet performing a roll motion around a generating gear axis perpendicular to the gear's pitch cone has become possible with Phoenix machines. The result is a perfectly conjugate interaction between pinion and gear, like shown in the contact analysis in Figure 2. The ease-off topography is zero and the tooth contact extends over the entire working area. The motion transmission error has a slight numerically caused variation but is practically zero. To prepare a gear set for manufacturing tolerances and deflections under load, length crowning can be created with a dished cutter as shown in Figure 3 and profile crowning can be created with a second order ratio of roll modification (Figure 4 bottom graphic).

For Related Articles Search
differential gears
at geartechnology.com

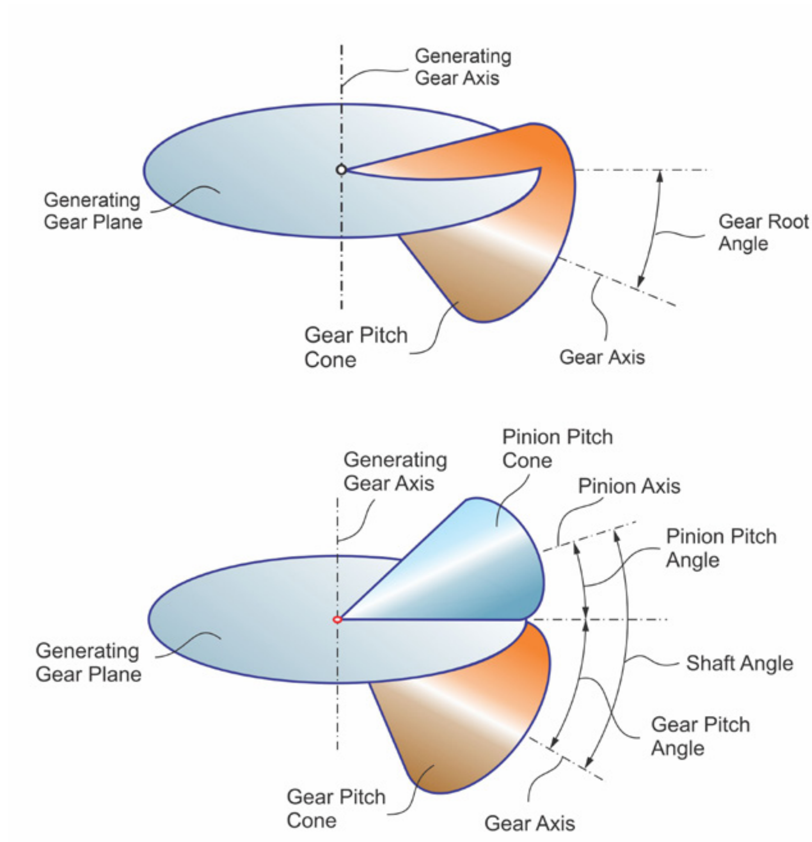

Figure 1—Coniflex Pro pinion and gear rolling on the pitch plane.

Tip Relief

The tooth profiles of a high-power density differential gear set should be conjugate in the center and feature a pre-determined tip relief. A new function in Coniflex Pro allows creating a higher order tip relief which preserves a low transmission error and protects better against edge contact as the traditional circular profile crowning. A typical Coniflex Pro tooth contact analysis is shown in Figure 5. The Ease-Off has higher order relief areas along tip and root. The flank center around the Mean Point is nearly conjugate and the tooth contact is full and centered. The motion transmission graph in Figure 5 shows very small amplitudes of 25 µrad (compared to the traditional 300 to 2,000 µrad).

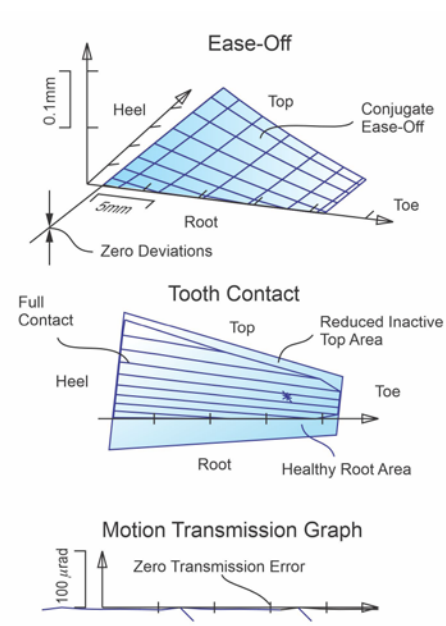

Figure 2—Contact analysis of Coniflex Pro gearset without crowning.

Double Positive Profile Shift

Until now, in bevel and hypoid gears, the same amount of positive profile shift used to reduce pinion undercut had to be applied to the gear, but with a negative sign. This was required to maintain the desired shaft angle. For differential gears, where the gear has also a low number of teeth, the profile shift had to be limited to small amounts to avoid undercutting the gear teeth. The newly developed independent profile shift allows positive profile shift for pinion and gear which results in stronger tooth profiles and increases the contact ratio by up to 50 percent. The principle is shown in Figure 6. Pinion and gear pitch cones are smaller by the equivalent amount of desired profile shift which reduces the shaft angle: $\Sigma_1 - X_{\gamma 1} - X_{\gamma 2} = \Sigma_2$ (Figure 6 left side). After the profile shift is applied, the reference pitch cones (working pitch cones) include the correct shaft angle Σ_1 (Figure 5 right side) and the gear set has the advantages of a positive profile shift in both members. To demonstrate the dramatic improvement of this technology, the tooth contact of a differential gear set without profile shift is shown in Figure 7. The tooth contact of the same gear set with double positive profile shift $X_1 = X_2 = +0.7$ is shown to the right in Figure 7. The contact pattern increased in profile direction by about 30 percent. The result is an increased contact ratio, a reduced root bending stress and a reduced flank surface contact stress.

Stress Comparison Coniflex Pro vs. Forged

A root bending stress and surface stress comparison between Coniflex Pro cut and forged gears was performed with the *ANSYS Finite Element Method.* The Coniflex Pro differential gear set was designed to replace the originally forged version. Also, a model of the side gear spline was created, and the input torque was transmitted from the splined shaft via the internal spline in the side gear bore to the side gear teeth. A torque of 1,000 Nm, which reflects the duty cycle peaks of a midsize EV, was applied. The bending stress results to the left in Figure 8 show a considerable advantage of the cut side gear (i.e., the cut pair). It is noticeable by the red patch inside of the web area at the toe that the web restricts the necessary tooth deflection in this critical area, resulting in twice the bending stress of the cut gear. The high load contact area in the right-side graphics (red) fades out smoothly on the Coniflex Pro cut gear but extends to tip and root on the forged version. This proves the advantageous function of the Coniflex Pro tip relief. Also, the contact stress magnitudes in Figure 8 show up to 65 percent higher values of the forged gear. The especially the high value of 3753N/mm² in connection with the high bending stress in the same area will result in high sub surface stresses which can cause case crushing. Case crushing often leads to flank fracture.

Also, an interesting result is the lower load sharing with neighboring tooth pairs of the forged gear set which reduces the effective contact ratio. In

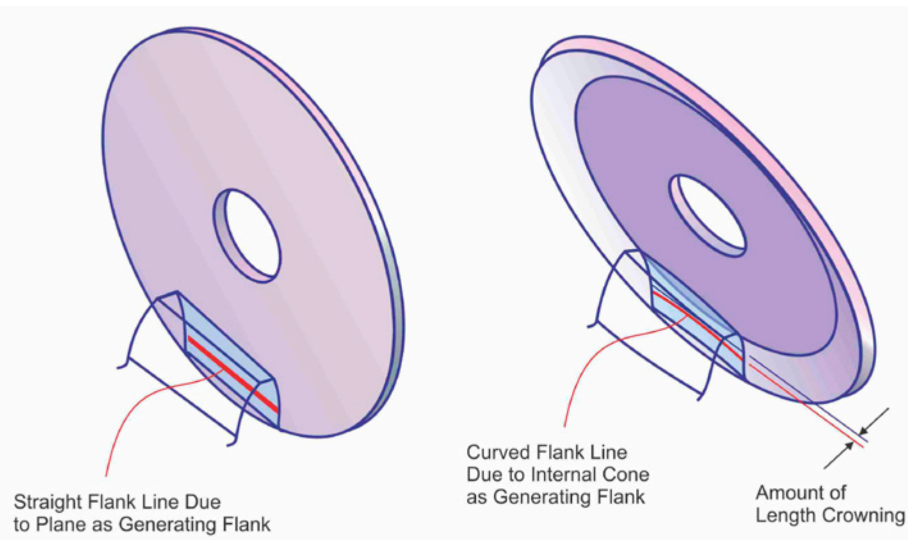

Figure 3—Length crowning is created with a dished cutting or grinding tool.

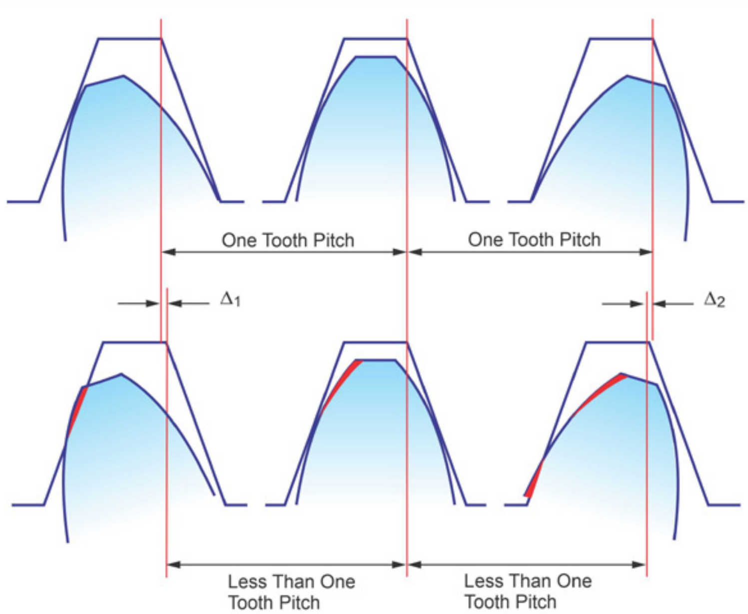

Figure 4—Conjugate generating (top) and generating of profile crowning (bottom).

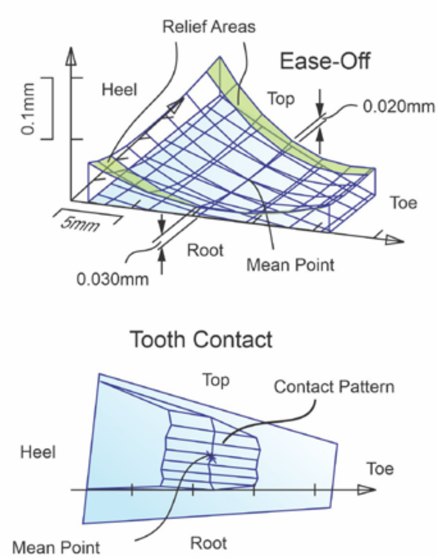

Figure 5—Coniflex Pro gearset with length crowning and kinematic top and root relief.

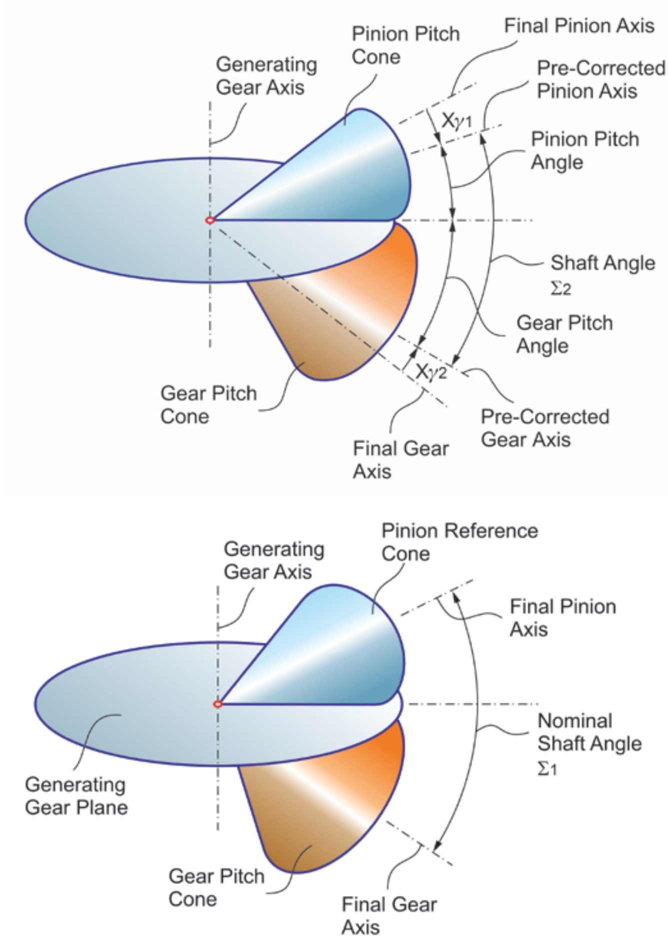

Figure 6—Contact analysis of Coniflex Pro gearset without crowning.

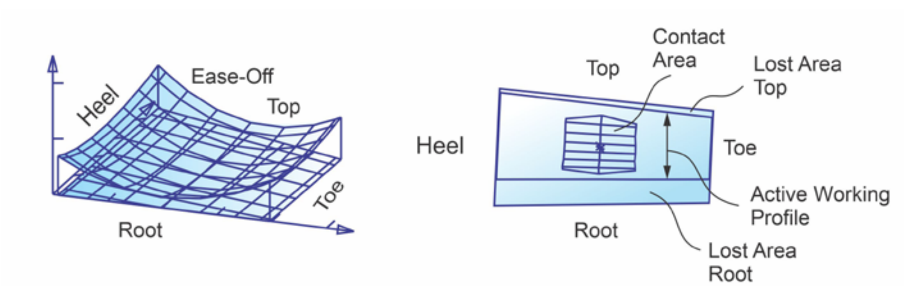

Figure 7—Contact analysis Coniflex Pro without profile shift (left side) and with double positive profile shift (right side).

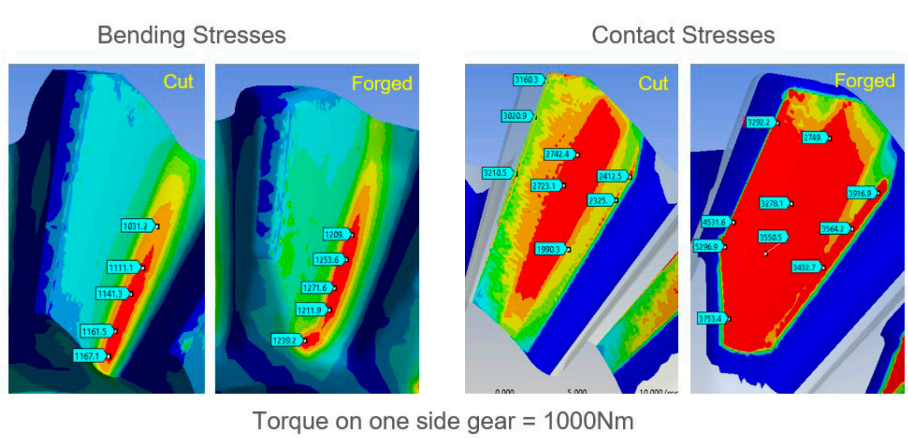

Figure 8—Stress comparison, Coniflex Pro cut versus forged (side gear torque = 1000 Nm).

Figure 9, a comparison of the load sharing for the Coniflex Pro cut differential gear set (bottom graphic) with its forged predecessor (top graphic) is presented. The green graphs in Figure 9 have their maximum at the center of three consecutive tooth pairs. The periodic shape of the graphs represents in the ordinate direction the contribution of load transmission of this particular pair of teeth in the current roll position (pitch position). The blue and the red graphs represent the two tooth pairs neighboring the tooth pair represented by the green graph. A vertical line in the upper diagram (at the center of the graphic) intersects the green graph at 80 percent and the red and blue graphs at 10 percent. This means that 80 percent of the input torque is transmitted by one pair of teeth. In the current example, the forged gear set has an effective contact ratio of 1:1 which means that on average 1:1 tooth pairs transmit the input torque at all times. A vertical line at the center of the lower diagram in Figure 9 (Coniflex Pro) intersects with the red and blue graphs at the 20 percent mark and with the green graph at the 60 percent mark. This means the maximal load the teeth have to transmit is 60 percent of the input torque because of the higher contribution of the neighboring tooth pairs. The effective contact ratio of the Coniflex Pro differential gear set in this example is 1:6.

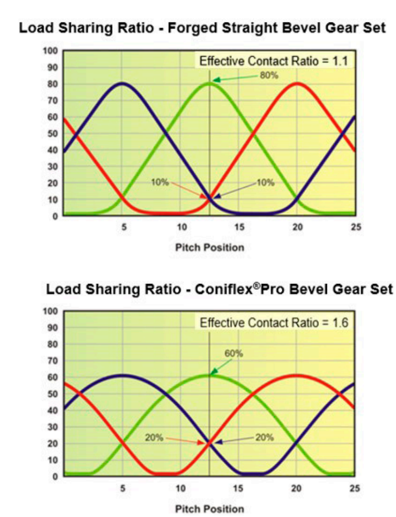

Figure 9—Comparison of load sharing and effective contact ratio (50 percent of nominal load was applied).

Transmission Error and NVH Comparison

With the *ANSYS Finite Element* software, the sample gear sets (cut and forged) have also been analyzed regarding motion transmission error under load. Figure 10 shows the results of the transmission error for the noise critical side gear torque of 40 Nm. The solid blue graph shows the transmission errors of the Coniflex Pro differential, and the dotted red graph shows the results of the forged differential. The cut differential (blue graph) has a maximum transmission error of 155 µrad. For the forged counterpart, the maximal transmission error is 740 µrad which is about 5 times the amount of the cut differential. Fast Fourier Transformations (FFT) were performed from the motion transmission graphs in Figure 10. The results shown in Figure 11 present transmission error amplitudes versus orders of mesh. The forged gear set (Figure 11, right side) has 295 µrad amplitude at the first mesh harmonic, which is also more than 5 times the value of the Coniflex Pro cut gear set (Figure 11, left side). FFT results reflect operating noise and vibration (NVH) rather well, which confirms that the sample Coniflex Pro differential has the potential to operate quietly in contrast to the forged version.

Summary

Coniflex Pro is a new development of straight bevel gears which, in contrast to the original Coniflex process, takes advantage of the geometric and kinematic freedoms available in Phoenix free-form machines. The advantages of a conjugate base geometry and the free control of length and profile crowning with the possibility of a kinematic tip relief in connection with positive profile shifts in pinion and gear have been compelling facts for manufacturers of differential gears for electric vehicles. The number of Coniflex Pro EV differential gear designs is constantly increasing. Coniflex Pro differential gear sets can be designed and optimized in the Gleason *GEMS* software system. The tools used are Coniflex Plus stick blade cutters. Digital flank form data including correction matrixes can be transferred via network to coordinate measuring machines and a closed correction loop between measurement and manufacturing machine can be established. Also, the machine summaries for blade grinding, cutting, and grinding are generated in *GEMS* and can be transferred to the manufacturing machines via the network. Coniflex Pro differential gears can be ground after heat treatment. Standard differentials might, in extreme cases, see a maximum of 400 rpm relative speed between side gear and planet. For some EV drive concepts, the maximal relative differential speed is six times higher, which calls for a hard finishing operation after the heat treatment. *GEMS* also generates grinding summaries and grinding wheel geometry and design data. Cutter head and grinding wheel consolidation between different gear designs is easily possible because the profiles of blades and grinding wheels are simply straight. The major advantage of Coniflex Pro is the power density, which can be twice that of conventional differentials. The quiet rolling is a welcome additional advantage. Both the high power density and low NVH properties make the change from forged differential gears to Coniflex Pro very interesting, especially for modern electric vehicles.

gleason.com

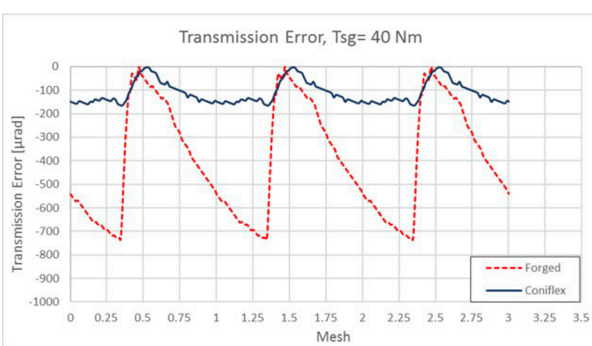

Figure 10—Comparison of the motion transmission error Coniflex Pro (blue) vs. forged (red).

Prof. Dr. Hermann J. Stadtfeld
Vice President Bevel Gear Technology and R&D, Gleason Corporation.

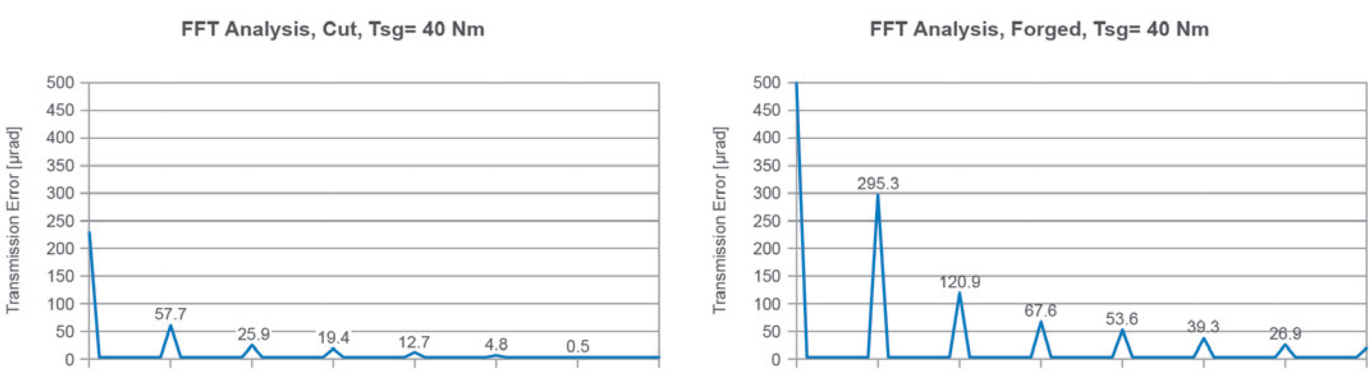

Figure 11—Comparison of Fast Fourier Amplitudes Coniflex Pro (left side) vs. forged (right side), side gear torque = 40 Nm.

The Outcome is Only as Interesting as the Process

Mary Ellen Doran, AGMA Vice President, Emerging Technology

The year has started strong for AGMA's Emerging Technology activities, with some of the highest registration numbers to date. (Recordings of all webinars are available for free at: *agma.org/events-education/on-demand-webinars*). I'd like to highlight our March webinar, where we debuted the committee white paper "The Near Future of Mechanical Drive for Humanoid Robots" alongside a panel of experts who contributed to it.

The paper examines the recent surge in investment, projections, and technological advancements in humanoid robotics over the last eight months of 2024. Its primary focus is how the mechanical components market could be impacted if these ambitious forecasts come to fruition, especially in actuators and gearboxes.

Special thanks go to the paper's author, Jacques Lemere, Principal at PBD Consulting, and the Robotics Committee Chair, Robert Kufner, President and CEO of SDP/SI–Designatronics, Inc., along with the content specialists and Robotics Committee members who provided valuable input throughout the process.

One of the highlights of my role is the off-camera conversations during committee meetings. At our most recent Robotics Committee meeting, one member made a compelling point: it's unlikely that one machine can handle every task. Drawing from his expertise in consumer products, he noted that we don't design products to do everything. Expecting humanoid robots to walk on two feet and handle tasks as varied as folding clothes and assisting elderly parents is like designing a car to drive, fly, and float—it's inefficient. The discussion was lively, with some passionate comments, and I left with greater insight. I'm grateful to the committee members for their time and expertise. I encourage you to join us for a committee meeting to contribute to these important discussions.

The paper addresses two key questions:

What will it take to meet the production numbers forecasted in recent economic reports?

How can manufacturing scale to meet these demands, particularly regarding gear components?

It starts with a brief history of humanoid robots and the evolution of drive components used in biped models. It then outlines two major differences between humanoid and industrial robots:

Power Source—Humanoid robots will be battery-powered, unlike DC-motor-powered industrial models.

Backdrivability—Since humanoid robots will interact with humans, safety is crucial. Consumer product laws will guide these requirements.

The paper also explores current gearbox designs in humanoid systems and how they may need to evolve. It examines emerging technologies that could address these challenges, including plastic gears, nanocomposite coatings, integrated actuation systems with low gear ratio planetary gears and affordable mechanical joints.

AGMA's Emerging Technology initiatives continue to drive important conversations within the robotics community. The white paper provides a thorough examination of the rapidly advancing humanoid robotics sector and its potential impact on mechanical components. The passionate discussions at committee meetings underscore the complexity of balancing technological innovation with practical, cost-effective solutions. As the industry moves forward, key challenges such as safety, reliability, and cost must be addressed to enable the successful deployment of humanoid robots.

The secret to a great committee meeting is passionate conversation. We encourage you to engage with these discussions and help shape the future of humanoid robotics by joining future webinars and committee meetings.

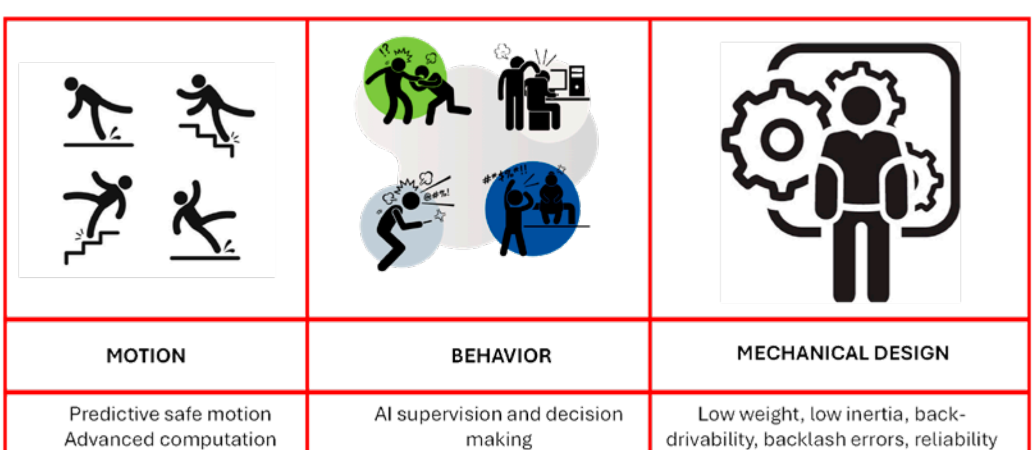

Humanoid failure categories.

GMTA German Machine Tools of America

Profilator QUALITY MEETS SPEED

OUR LINE JUST GOT LONGER...

Looking for a partner for your green and hard finishing operations?

GMTA now offers a broad assortment of machine tool technologies for both green and hard machining of gears and other power transmission related components. Our product portfolio consists of horizontal and vertical turning, the patented **Scudding** process for gear internals and externals, horizontal and vertical gear hobs, cylindrical grinders, gear generating grinders, and gear honing machines. Whether you are sourcing a single process or a turn-key system, we've got you covered.

Plus enjoy the advantages of **GMTA** application engineering, unmatched experience in the manufacturing technology of gears and other power transmission components, multinational support in sales and service, plus the unique assortment of machine tools and related equipment to keep your process at peak efficiency.

See our machines in action!

Profilator – Scudding (Skiving)

Seiwa – Gear Hobbing

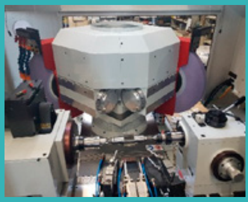

MAR – Universal Cylindrical Grinding

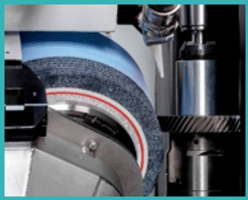

Toyo – Gear Generating Grinding

emco SEIWA G-TEC INC. MAR GRINDING MACHINES TOYO

4630 Freedom Drive | Ann Arbor, MI 48108 | +1 734-973-7800 | www.gmtamerica.com

Gears for the toughest machines on earth.
Together, we are the force that moves the world.
We offer a wide variety of manufacturing capabilities covering almost the entire powertrain and driveline applications.
We make available one of the widest production capability for custom gears for heavy duty vehicles of the entire industry to enable our O.E.M. Customers to focus more on their projects.
IATF 16949 and ISO 14004 Certified
CATTINI NORTH AMERICA
www.cattinina.com
Pedetemptim sed incessanter®

Nidec
Expert gear cutting tool and broach service
FEDERAL BROACH & MACHINE COMPANY
SOUTHEAST BROACH
= Fast turn around for your cutting tools
Sharpening and strip/recoat service for: hobs, shaper cutters, skiving cutters, shave tools, and broaches of all kinds.
TWO LOCATIONS TO SERVE YOU:
Harrison, MI Greer, SC
• FAST TURNAROUND
• IN-HOUSE COATING
• EXPERT EDGE PREP
• MAXIMUM TOOL LIFE
• HIGHEST PART QUALITY
CONTACT US TODAY!
rfq@federalbroach.com
989-539-7420
www.federalbroach.com

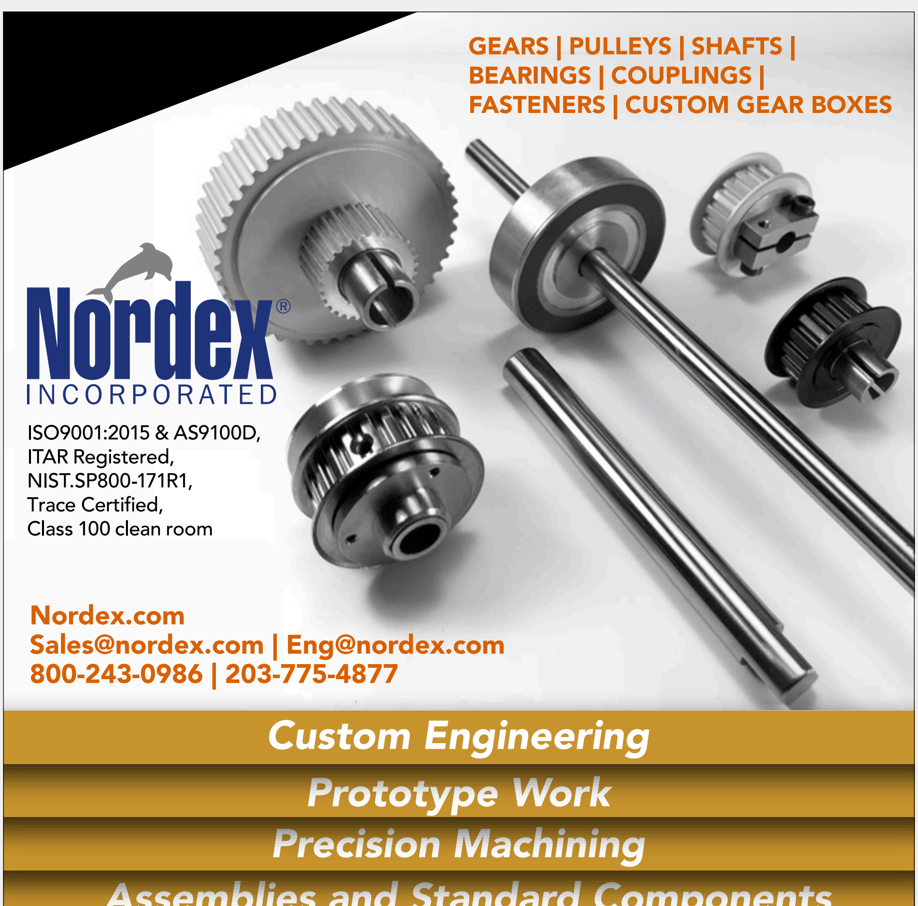

GEARS | PULLEYS | SHAFTS | BEARINGS | COUPLINGS | FASTENERS | CUSTOM GEAR BOXES
Nordex® INCORPORATED
ISO9001:2015 & AS9100D, ITAR Registered, NIST.SP800-171R1, Trace Certified, Class 100 clean room
Nordex.com
Sales@nordex.com | Eng@nordex.com
800-243-0986 | 203-775-4877
Custom Engineering
Prototype Work
Precision Machining
Assemblies and Standard Components

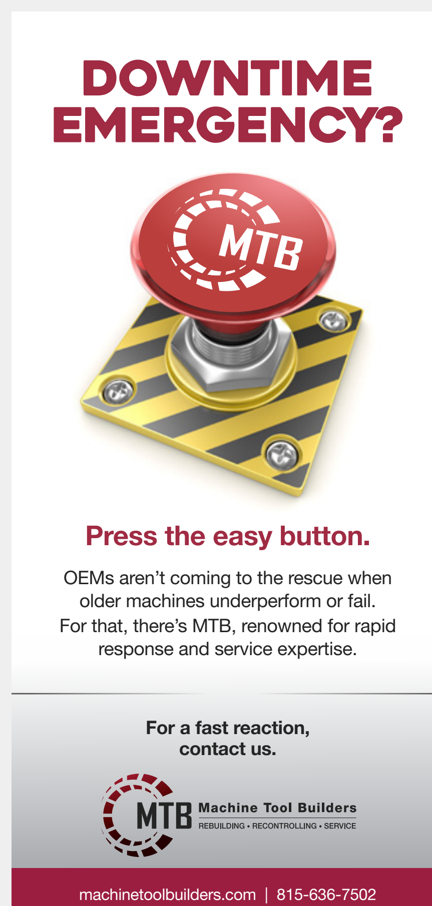

DOWNTIME EMERGENCY?
MTB
Press the easy button.
OEMs aren't coming to the rescue when older machines underperform or fail. For that, there's MTB, renowned for rapid response and service expertise.
For a fast reaction, contact us.
MTB Machine Tool Builders
REBUILDING • RECONTROLLING • SERVICE
machinetoolbuilders.com | 815-636-7502

Manufacturing sMart

Your resource for the latest in great ideas from our advertisers. Check this section every issue for sMart Engineering ideas and technology.

FOR INFORMATION ABOUT ADVERTISING CONTACT

Dave Friedman
Associate Publisher &
Advertising Sales Manager
friedman@agma.org
(847) 437-6604

The AGMA Fall Technical Meeting Process

Courtney Carroll, Senior Manager, Technical Services

AGMA's Fall Technical Meeting (FTM) is the best place in the U.S. to share gear manufacturing research. If you want to write a paper and present, here is how it works.

AGMA uses an online portal to streamline the process. Because we have less than a year for the entire cycle—from abstract submission to publishing the paper—we must have firm deadlines.

Call for Papers. Whether it originates in your company's R&D department or is included in your school's research objectives, share your research! We look for material that is at the right level for FTM (not too simplistic); not too commercial; original subject matter (although an expansion on previous research is acceptable); and relevant to the gear manufacturing industry.

Through the online portal, authors submit 200–300-word abstracts. Presenters must be able to travel to the United States to present in person for the paper to be published.

The committee managing the FTM program consists of engineers in the industry. They review the abstracts according to the above criteria (they do not know the identity of the authors). The abstracts are rated, and the top 30 are discussed for selection. If there are too many abstracts for one subject, the lowest-rated submission in that topic is removed. Keep in mind that abstract acceptance or rejection is not a personalized decision.

Once the committee decides which abstracts to accept, emails go out to authors, notifying them of their abstract's acceptance or rejection. If not selected for the FTM, we try to involve our authors as either an emerging technology presentation or article in *Gear Technology* or *PTE*.

Review draft. For accepted abstracts, authors have approximately three months to write their paper. This paper must be complete with all research and analysis so peer reviewers can provide a comprehensive review, and authors should use the provided FTM paper template.

During this phase, authors will sign a license agreement that gives AGMA the right to publish, sell, and distribute the paper. The author(s) retain the rights of ownership of the paper. AGMA also needs the speaker's biography and photo and a shortened version of the abstract for marketing.

Peer review. AGMA requires peer review for technical papers to ensure relevance, accuracy, and reliability of the research. Engineers in the industry volunteer to review the papers. The committee then chooses three subject matter experts to review each paper. Peer reviews are double-blind to prevent bias, so the peer reviewer does not know the identity of the author, and vice versa.

The selected peer reviewers then rate the paper for each criterion:

- Introduction and body of the paper clearly states objective(s).
- Supporting materials (equations, data, graphs, figures, tables) are relevant, accurate, and clear.
- Conclusion is supported by presented material and answers the stated objective(s).
- The paper is free of commercialism and does not promote a company or any system, process, tool, machine, material, or software specific to a company.

Peer reviewers then give an overall acceptance recommendation: approve as-is or with editorial comments only; approve with substantive technical comments; or disapprove. If you'd like to be a peer reviewer and have technical expertise, please contact *ftm@agma.org*.

If two of the three peer reviewers disapprove, the paper is assessed to see if it can be edited. If the paper needs substantive changes, AGMA contacts the author to see if he or she can make the necessary changes. If so, the author receives all peer reviewer feedback and verifies how they will change the paper to meet the criteria.

Final paper. The peer review results (for those papers not needing substantive changes) are then available, and the authors have about two months to make final edits to the paper. An AGMA staff then finalizes the paper for distribution.

PowerPoint presentation. Finally, authors submit their PowerPoint. Presenters should practice their presentation ahead of time to stay within their 20-minute time at FTM.

And that's the process!

The Role of In-Situ Techniques in Microstructure Optimization of Interstitially Alloyed Steels

Qianchen Zeng, Ellen Troyanosky, Noah Kantor, Jianyu Liang, Thomas L. Christiansen

Introduction

Various in-situ methods can track real-time heat treatment response in bulk materials. This can aid material engineers in designing the most effective heat treatment procedures and processing methods. In-situ methods such as thermogravimetry (TG), differential thermal analysis (DTA), and dilatometry, offer capabilities to examine heat treatment behavior in real time, giving insight into the thermochemical mechanisms and the thermal behavior of steel.

This contribution specifically addresses different martensitic (stainless) steel where in-situ control during heat treatment and detailed understanding of their microstructure can pave the way for new applications. The examples presented are 1) heat treatment behavior of different classes of high carbon martensitic (stainless) steel powder for additive manufacturing application, i.e., stainless 440C, cold-work D2, hot work H13, and high speed steel (HSS) T15, 2) nitrogen alloying of wrought martensitic stainless steel AISI 420, and 3) heat treatment response of additively manufactured and conventional precipitation hardening maraging stainless steel 17-4PH. This work is not an in-depth treatise of these individual topics but is intended to show the importance of in-situ techniques for development of new materials (solutions). The individual topics are briefly introduced in the following.

High Carbon Steel Powders for Additive Manufacturing

Additive manufacturing (AM) is gaining popularity and experiencing rapid technological advancements. Recently, there has been a significant focus on the application of high-carbon steels (Ref. 1). AM methods, such as laser powder bed fusion (LPBF), binder jetting (BJ), and spray forming, offer several benefits, including the attainment of uniform microstructures which offer superior mechanical properties compared to conventionally manufactured metals. Currently, several specialized high-carbon powders are now commercially available for AM. For a successful adoption of high carbon steels for AM, more knowledge on the fundamental thermal behavior related to the processing is needed. To this end, powders and in-situ techniques are an excellent foundation for investigating heat-treating characteristics.

440C stainless steel (440C) is a high-carbon martensitic stainless steel known for its high hardness, wear resistance, and moderate corrosion resistance. According to Bang et al. (Ref. 2), LPBF addresses the limited industrial applications caused by 440C's high hardness and low workability, while also improving overall mechanical properties such as ultimate tensile strength (UTS) and yield strength (YS) (Refs. 4,5).

D2 cold-work steel (D2) is distinguished by its superior hardness, high strength, and excellent wear resistance, making it widely used in industrial applications like cutting and punching tools, as well as dies. This material is well-suited for AM techniques, particularly direct energy deposition (DED) (Ref. 5). H13 hot-work tool steel (H13), typically utilized in a quenched and tempered state, features a martensitic matrix with dispersed fine secondary carbides. Known for its high hardness and fracture toughness, H13 also offers excellent wear and erosion resistance, along with relatively high resistance to thermal shock and thermal fatigue. As noted by Park et al. (Ref. 5), metal deposited via the DED process exhibits different properties compared to wrought metal due to the rapid solidification rate and the high thermal gradient between the deposited metal and the substrate. The microstructure of deposited D2 and H13 has been shown to be highly uniform, with the hardness of deposited D2 comparable to conventional martensitic high-carbon stainless steel, and the hardness of deposited H13 exceeding that of wrought H13.

T15 high-speed steel (T15) is well known for its high hardness and

First presented at the 2024 Fall Technical Meeting (FTM), October 7–9, 2024, Rosemont, IL. Printed with permission of the author(s). Statements presented in this paper are those of the author(s) and may not represent the position or opinion of the American Gear Manufacturers Association.

excellent wear resistance at elevated temperatures, attributed to its significant carbon and tungsten content, making it an ideal material for cutting tools, drills, blades, and knives. According to Zhang et al. the spray-formed T15 steel exhibits higher hardness, significantly enhancing its overall mechanical properties (Ref. 6). This increase in hardness is a crucial factor contributing to the superior mechanical performance of T15 steel in various applications (Refs. 8–11).

Nitrogen Alloying to Martensitic Stainless Steel; High Temperature Solution Nitriding

Adding nitrogen to stainless steel may be beneficial to the bulk properties of the material, such as increased surface hardness and optimized microstructures that retain the corrosion resistance. Nitrogen can be added in the liquid phase during fabrication of the steel, but this is usually an expensive and cumbersome process as it requires high N_2 pressures and there is the risk of formation of nitrides during cooling and subsequent processing. An alternative is "High Temperature Solution Nitriding" (HTSN), where nitrogen is introduced from the gas phase to the solid state—a process which is highly analogous to classical carburizing of non-stainless steels. Nitrogen is typically added to stainless steels at temperatures ranging from 1,050–1,150°C and using pressures of N_2 ranging from 0.1 to 3 bar (Refs. 11,12). The process entails gas quenching in N_2 to suppress formation of chromium nitrides. The entire process is carried out in a clean environment and will provide improved corrosion resistance, higher hardness and wear resistance and enhanced fatigue performance. The process is particularly interesting for martensitic stainless steels but can also be applied to austenitic and duplex stainless steels. Depending on a wide variety of process conditions, some being the alloy content, nitrogen pressure and the subsequent cooling rate, the resulting final microstructure can vary quite significantly. Additionally, the total amount of nitrogen taken up by the material will also impact the final microstructure, for example the phases developed (viz. martensite) and the morphology of martensite (Ref. 13). Adding nitrogen through HTSN to martensitic steels can come at a cost. Since nitrogen itself is a strong austenite stabilizer, this can produce higher amounts of retained austenite following quenching, which many times are undesirable (Refs. 14,15).

The complexity of diverse alloying elements and process conditions means that process optimization can be tedious and require many iterations. The interplay between retained austenite and solution hardening associated with martensitic stainless steels is considered through the analysis of sample microstructures of the investigated materials. In-situ methods offer the benefit of completing lab scale iterations, achieving fast results in a clean and controlled environment. As mentioned previously, the HTSN treatment can produce "case-hardening-like" results. The discussed in-situ techniques can be applied to other traditional gaseous case hardening processes such as carburizing of steels, where similar uptake behavior is present.

17-4 Precipitation Hardening Steel

Precipitation hardening (PH) steels, such as 17-4PH, are martensitic stainless steels that harden through forming precipitates during an aging treatment. The standard heat treatment for 17-4PH for peak hardness is the 900H treatment, involving a solution treatment around 1040°C, quench, then age around 480°C (≈900°F) for one hour (Ref. 16). 17-4PH primarily forms Cu precipitates in the martensite phase, so when the quenching fails to complete the martensite transformation, retained austenite will limit the hardness of the final material (Ref. 17).

In AM, LPBF 17-4PH can have a primarily austenitic structure due to N_2 gas-atomized powders and N_2 cover gas used during processing. In addition to the austenite stabilizing effects of nitrogen, LPBF 17-4PH tends to have a cellular or dendritic structure associated with microsegregation of the alloying elements. This further suppresses the martensite transformation, leading to a primarily austenitic microstructure after heat treatment.

Like other AM metals, the unique composition and microstructure of LPBF 17-4PH requires a modified heat treatment to achieve the desired material properties. Other studies have found success in lowering the solutionizing temperature (Ref. 17), extending the aging time (Ref. 18), or incorporating sub-zero Celsius treatments (Ref. 19).

Experimental Procedures

Materials

The high carbon steel powders investigated were delivered from Asgaard Metals and were overspray from spray forming of ingots. The compositions, as provided by the supplier, are given in Table 1.

AISI	Fe	C	Cr	Mn	Si	Mo	Co	V	P	Ni	Cu	S	W
SS440C	Bal.	1.1	17	1	1	0.75	-	-	0.03	0.3	0.25	0.03	-
D2	Bal.	1.4-1.6	11-13	0.6	0.6	0.7-1.2	1	1.1	0.03	0.3	0.25	0.03	-
H13	Bal.	0.32-0.45	4.75-5.75	0.35-0.6	0.8-1.2	1.1-1.75	-	0.8-1.2	0.03	0.3	0.25	0.03	-
T15	Bal.	1.5-1.6	3.75-5	0.15-0.4	0.15-0.4	1	4.75-5.25	4.75-5.25	0.03	0.3	0.25	0.03	11.75-13

Table 1—Steel powder composition in wt% (as-received).

For Related Articles Search
metallurgy
at geartechnology.com

Rods of AISI 420 stainless steel with the diameter of 12.7 mm from McMaster-Carr were used. The material was received in the hot rolled and cold annealed state. The composition as provided by the supplier is listed in Table 2. The rod was cut using a precision saw into a 5 mm thick disk to be used for thermogravimetric measurements.

Wrought 17-4PH samples, 5 mm diameter rods supplied from McMaster-Carr in a cold-worked, solutionized and unaged state were used. LPBF samples were produced by GKN using their nitrogen gas-atomized ANCOR AM 17-4PH powder. The composition of 17-4 rods and powder is given in Table 3. The LPBF set was made using standard parameters with an N_2 cover gas. For dilatometry, rods of 10 mm length and 5.5 mm in diameter were machined with the long axis parallel to the building direction. The rods were then cut into bars of 10 mm in length.

Thermal Gravimetry (TG) and Differential Thermal Analysis (DTA)

Both TG and DTA results were obtained using the Netzsch STA 449 F3 Thermal analyzer. For TG analysis of AISI 420, a 2.9 g round bottom alumina crucible was utilized. The sample was positioned with one flat side facing upwards. This crucible was measured as having a 15.75 mm internal diameter. Samples of high carbon stainless steel powders were poured into flat-bottom alumina crucibles with an internal diameter of 6.00 mm and an internal depth of 3.75 mm. The flat bottom crucibles were filled around three-quarters of their maximum capacity. Immediately following the purge cycle of inert gas, these crucible samples were placed onto the sample holder in the furnace compartment. For each thermal analysis, the furnace chamber and balance system were put under vacuum and then backfilled with argon or nitrogen. The furnace chamber was then heated according to the specific temperature program set. The main parameters set can be seen in Table 4. The nature of the performed experiments is indicated in the table.

Dilatometry

Dilatometer tests were run on the TA Instruments DIL805 following the peak hardening treatment for 17-4PH. Under vacuum, 1,037°C for 3 h, followed by a quench to room temperature in He gas at a rate of -33.6°K/s. It is then aged at 482°C for 1 h under vacuum and then quenched.

Metallography

Samples were cut using a Buehler IsoMet High Speed Pro precision saw to obtain cross sections for examination. Blades were chosen to fit the specific material being cut. Each sample was mounted in a Buehler Simplimet 4000 mounting system, using Buehler PhenoCure compression mounting compound. All mounted samples were polished on the Buehler AutoMet 250 according to Buehler's standard 4-step method for stainless and maraging steel polishing. Samples were then etched using Kalling's reagent, which consists of 33 percent hydrochloric acid, 33 percent ethanol, 33 percent deionized water, and 1 percent cupric chloride dihydrate. The samples were swabbed for approximately 5 seconds, terminated with deionized water, and cleaned using ethanol. Micrographs were obtained using a Nikon Epiphot 200 Microscope. Vickers hardness tests were completed using the Wilson VH3300 automated hardness tester using a load of 0.5 kg, and a 10 s dwell time.

X-Ray Diffraction (XRD)

XRD analysis using a PANalytical Empryrean x-ray diffractometer. For 17-4PH Cr K-α radiation with wavelength 2.28976 A was applied. For the

Fe	C	Si	Mn	Cr	Mo	Cu	Ni	Al	P	S	Sn
Bal.	0.31	0.44	0.68	12.66	0.04	0.10	0.25	0.004	0.017	0.026	0.006

Table 2—AISI 420 composition in wt% (as-received).

	Fe	Cr	Ni	Cu	Mn	Si	Nb	C	S	N
Wrought	Bal.	15.20	4.28	3.66	0.92	0.39	0.26	0.04	0.021	0.027
Powder	Bal.	16.5	4.5	3.9	0.4	0.3	0.3	0.01 (max.)	0.02 (max.)	0.05 (max.)

Table 3—Composition of wrought 17-4PH in wt% as provided by the producer and the nominal composition (unless noted as a maximum) of the powder used to produce the LPBF samples. Values for powder composition are reproduced from Ref. 16.

Material	Atmosphere (gas, partial pressure)	Type/purpose of experiment	Heating Rate (°C/min)	Isothermal Hold Temperature (°C)	Isothermal Hold Time (HH:MM)	Cooling Rate (°C/min)
SS440C, D2, H13, T15	Ar,70ml/min	Isochronal heating/cooling; thermal behavior	10	1150	10:00	10
SS420	N2,50ml/min	Gradient of nitrogen by high temperature solution nitriding (isothermal)	20	1100	10:00	20
Wrought 17-4PH	N2,92ml/min,Ar,8 ml/min: 5 h N2,5.5ml/min,Ar86 ml/min: 13 h	Synthesis; controlled addition of nitrogen (homogenously)	10	1150	16:00	30

Table 4—Thermal analyzer conditions.

high-carbon steel powder, XRD analysis was done using Cu K-α radiation from 30 to 125 2θ angle, with a step size 0.03 degree and step time 15 s. The results were analyzed using Origin and the recorded line profile was smoothed by using Savitzky-Golay method.

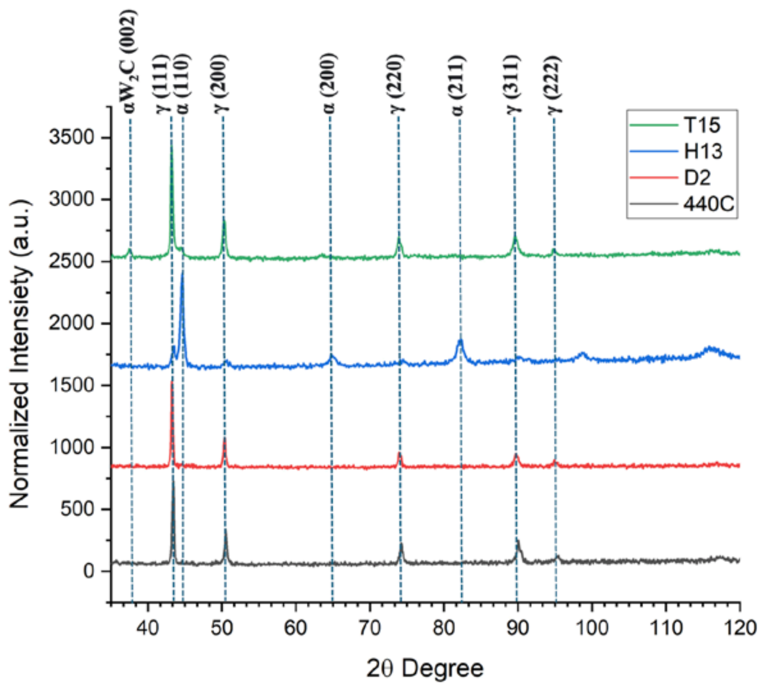

Figure 1—XRD patterns of as-received overspray powders 440C, D2, T15 and H13.

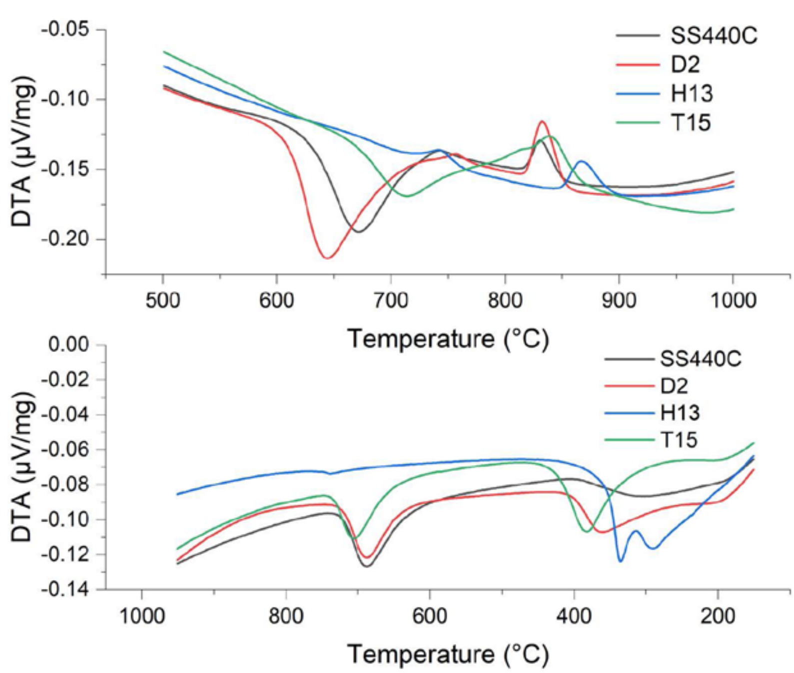

Figure 2—DTA of overspray alloy powders 440C, D2, T15 and H13 during heat and cooling with 10K/min and with an austenitization temperature of 1150°C (holding time 10 min.). Heating (top) and cooling (bottom).

Results and Discussion

High Carbon Martensitic Steel Powders

The overspray high carbon steel powders are unique in the way that they are a byproduct from spraying of steel ingots, i.e., they are rapidly solidified and cooled. Hence, the microstructure is not necessarily conventional, which emphasizes the importance of in-situ tracking of their thermal behavior.

XRD analysis of the as-delivered powders are given in Figure 1. The materials 440C and D2 are fully austenitic which can be attributed to fast cooling (inherent to the process) combined with a high interstitial content. T15 is also predominantly austenitic with a minute fraction of ferrite/martensite; minor peaks of W_2C type carbides can also be observed. H13 is predominantly ferritic/martensitic with a minor fraction of (retained) austenite.

DTA during isochronal heating can record phase transformations or reactions associated with release or uptake of heat (calorimetry). Upon heating, the powders 440C, D2, and T15 undergo an exothermic reaction in the temperature range of 620-750°C, which can be attributed to (partial) decomposition of austenite, presumably via eutectoid decomposition, i.e., alloy pearlite. This transformation is most pronounced for 440C and least pronounced for T15, which correlates with the amount of retained austenite in the initial condition. A second peak, occurring between 800-900°C for all materials, is attributed to the formation of austenite (Ac1). Examination of the DTA signal (Figure 2) indicates that the austenitization start temperature for SS440C is approximately 820°C, with complete transformation at 850°C. For D2, austenitization begins around 820°C and completes at approximately 860°C. In the case of H13, austenitization starts at around 850°C and concludes at about 900°C. For T15, austenitization commences at around 810°C and is complete at approximately 875°C.

The calorimetry signals from cooling at a rate of 10 K/min are given in (Figure 2). The exothermic peak for the carbon rich SS440C, D2 and T15 indicates the eutectoid transformation of austenite into alloy pearlite occurring during cooling around 750–650°C, analogous to the transformation taking place during heating. The second peak in the DTA signal (for all alloys) during cooling indicates formation of bainite at around 375°C followed by martensite formation. This behavior is consistent with CCT diagrams of the conventional wrought materials (not shown herein).

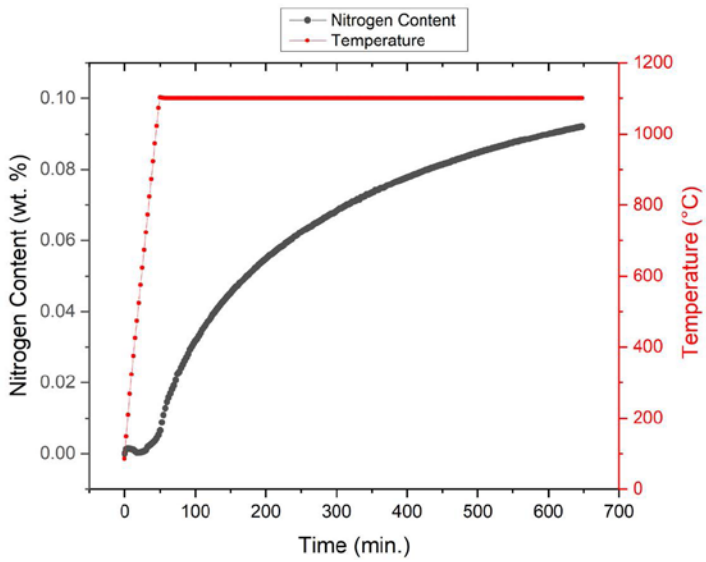

Figure 3—TG uptake during 10-hour HTSN of AISI 420.

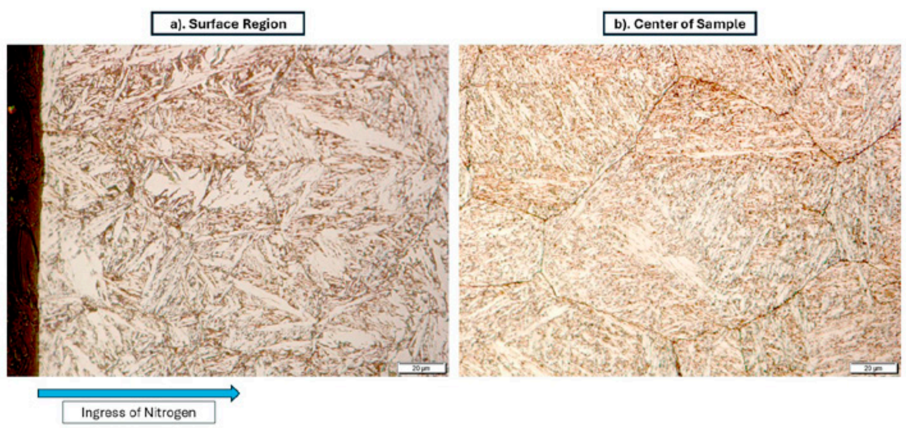

Figure 4—Micrographs of AISI 420 following a 10-hour HTSN treatment at the (a) surface region of the sample, (b) center of sample.

HTSN of AISI 420

To assess the role of nitrogen in martensitic stainless steels, high temperature solution nitriding can be used, which will result in a graded structure provided the sample is not through-nitrided. Herein, the widely used AISI 420 is selected to illustrate the impact of nitrogen on the microstructure. Please note that the solution nitriding temperature of 1,100°C coincides with the conventional temperature for austenitization of this material. The applied cooling rate from the nitriding temperature is relatively slow, but here it is merely to demonstrate the effect of nitrogen rather than to present an optimized process. Figure 3 depicts the results obtained for in-situ gaseous nitriding through TG analysis. This graph represents the temperature and mass uptake of nitrogen in the sample. As can be observed in the figure, the total sample uptake prior to cooling comes to approximately 0.09 wt% nitrogen. The flux of nitrogen follows directly from the in-situ recorded uptake of nitrogen during nitriding, when considering the specimen's surface area. The overall nitriding kinetics seems to follow a parabolic growth law indicating diffusion-controlled growth rather than growth governed by surface kinetics. It should be noted that the weight percentage of nitrogen is measured in the entire sample, with a diffusion gradient of interstitial nitrogen moving from high concentration at the edge to a lower concentration at the center according to Fick's second law of diffusion (Ref. 20). Hence, the surface region of the sample has a significantly higher nitrogen concentration than the overall 0.09 wt%, whereas the core has essentially no nitrogen.

Micrographs at different magnifications were obtained from two regions of the 420 stainless steel, adjacent to the surface where the nitrogen concentration is highest and at the center of the sample. Figure 4 (a.) represents the surface region of the 420 stainless steel disk and Figure 4 (b) represents the center of the disk, which is essentially without nitrogen, but contains carbon.

As shown in the micrographs (Figure 4), there is a noticeable difference in the grain structure and phases within the sample. Due to the transient nature of this gaseous process, it can be inferred that there is a higher concentration of nitrogen near the surface of the sample, which was in contact with the gaseous atmosphere. In Figure 4 (a), the grain structure can be seen to be finer, albeit with larger martensitic plates. These plates can be identified by their white color. Figure 5 shows a closer view of this morphology which appears to be lenticular or thin-plate martensite and it has a characteristic zigzag pattern. This type of morphology is related to an increased nitrogen content (Refs. 21,22). It could be inferred that the dark portions indicate the presence of some form of nitride, likely chromium nitrides, which decorate the outer grain boundaries.

Figure 4 (b) shows much larger grains than can be seen in Figure 4 (a). This feature can be, in part, due to the absence of grain pinning in this region. Initial formation of nitrides will occur in the surface region during heating to the nitriding temperature (1,100°C); at the nitriding temperature, the nitrides will dissolve. The presence of chromium nitrides can pin grain growth near the surface where the nitrogen content is high (Ref. 21). The different composition of interstitial elements between case and core can also play a role for grain growth of the austenite. The micrograph indicates the presence of mainly lath martensite. Nitride formation should not take place, so the grain boundary decorations observed are likely carbides forming during cooling. The presence of nitrogen in this sample demonstrates an interesting relationship between solution hardening and retained austenite, where the former serves to harden the material, and the latter should soften the material when compared with martensite (Ref. 20). The higher the interstitial content in martensite, the greater the hardness. However, the higher the interstitial content dissolved in the austenite, the lower the martensitic start (M_s) temperature; therefore, more retained austenite is present. The greater the retained austenite fraction, the softer the material becomes. Here it should be mentioned that nitrogen and carbon have a significant solid solution strengthening effect in austenite; this effect is much more pronounced in stainless steels than in non-stainless steel. Another factor contributing to this balancing relationship is shifting the M_s temperature based upon the size of austenitic grains before martensitic transformation. A smaller grain size will lead to a lower M_s temperature; this effect works in conjunction with the nitrogen content. In terms of martensite morphology, higher nitrogen contents (lower M_s temperature), will result in a more plate-like morphology. Low nitrogen contents will be associated with a lath type martensite in this type of material (Ref. 23). Examining Figure 4 (b), the micrograph indicates the presence of lath martensite (Refs. 21,22) representative of a low nitrogen content.

Upon measuring the hardness of the HTSN treated 420 stainless steel sample, it is apparent that the hardness is relatively unchanged over the cross-sectional distance through the sample. Figure 6 shows reasonably stable hardness readings with the average hardness measuring at approximately 673 HV. This value is in the upper range of what is achievable based upon the carbon content in the sample. There is a slight dip towards the sample's edge which may be attributed to increased nitrogen content and higher fraction of retained austenite. Sub-zero treatment could be applied to minimize the amount of retained austenite.

When compared with the hardness of untreated 420 stainless steel, there is quite a significant hardness increase. The as-received hardness of 420 stainless steel in soft-annealed condition is approximately 200 HV. The hardness obtained from the HTSN treatment is quite similar to the hardness yielded by a traditional oil-quenched sample (approximately 610–740 HV) (Ref. 23). Using nitrogen, this maximum achievable hardness range can be extended.

For in-situ determination of M_s temperature, dilatometry can be applied but requires uniform nitrogen over the full

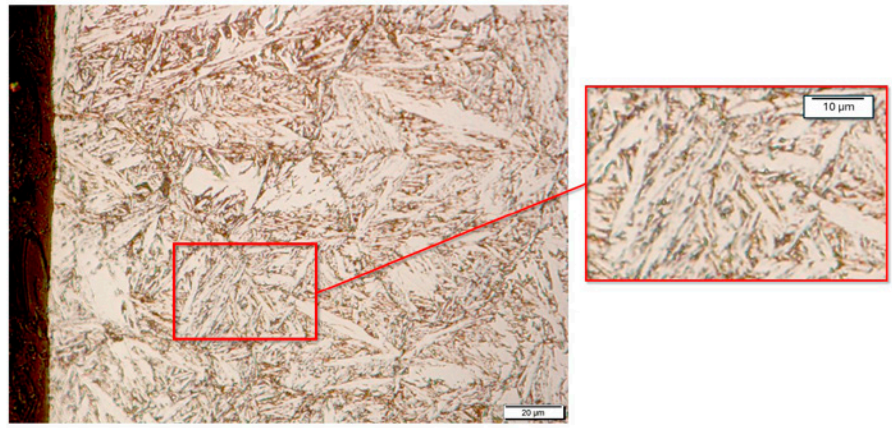

Figure 5—HTSN of AISI 420, Microstructure close-up at edge.

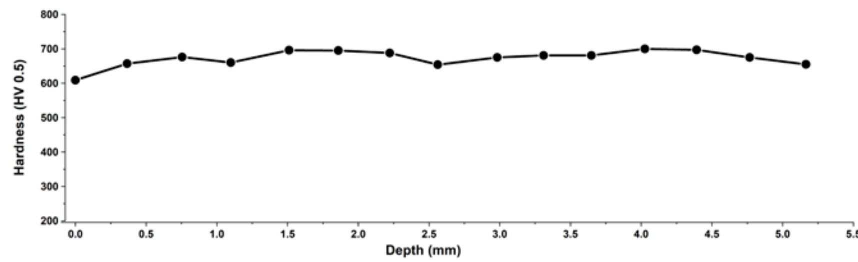

Figure 6—Hardness over the cross-sectional distance of AISI 420 stainless steel after a 10-hour HTSN treatment.

width of the tested sample. By using the in-situ thermal analysis, both HTSN processes as well as other traditional case hardening processes, could be refined. The unique feature of in-situ nitriding, carburizing, etc. is the ability to monitor the uptake kinetics as a function of time and/or temperature. The ability to carry out lab scale treatments in a controlled environment can save resources and allow for a more calculated and iterative approach to optimizing treatment.

Precipitation Hardened Stainless Steel

The wrought 17-4PH had a starting nitrogen content of 0.027 ± 0.0002 wt% N, the nitrogen-loaded wrought had 0.16 ± 0.004 wt% N, and LPBF had 0.13 ± 0.006 wt% N. Both wrought samples show similar slopes upon heating in the dilatometry curve (Figure 7) until a change in slope around 775°C, representing a phase transition. After quenching, both samples follow a new slope until a new change in slope at low temperatures, marking the martensite transformation. The point where this sharp transition begins can be labeled as the M_s temperature for that curve. The dilatometry curves for the wrought samples show that both started with a martensitic structure, transformed into austenite, represented by the steeper slope, and then transformed back into martensite. The LPBF curve maintains the steeper slope before and after quenching and shows no significant transformation curve. This suggests that the LPBF began with a primarily austenitic structure and did not reach its M_s temperature upon quenching.

The primarily austenitic structure is also reflected in the XRD results, plotted in Figure 8 below. Before heat treatment, LPBF displays intense austenite (γ) peaks and small ferrite (α) peaks. After heat treatment, the ferrite peaks become more prominent, but the austenite peaks remain, suggesting a partial martensite transformation. In comparison, the wrought 17-4PH has a completely martensite microstructure, as reflected by the intense ferrite peak.

Despite having a lower nitrogen content, the dilatometry curves show that LPBF remains austenitic for the entire heat treatment cycle while the nitrogen-enriched wrought starts and ends martensitic. This may be due to the anisotropic and dendritic/cellular structure characteristic of LPBF further suppressing the martensite transformation (Ref. 24).

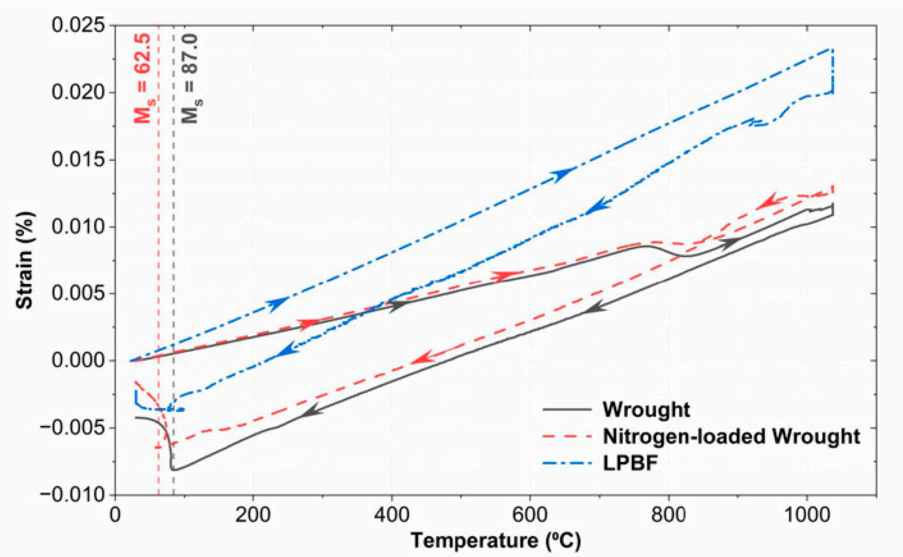

Figure 7—Dilatometry curves for the solution treatment of wrought, nitrogen-loaded wrought, and LPBF 17-4PH.

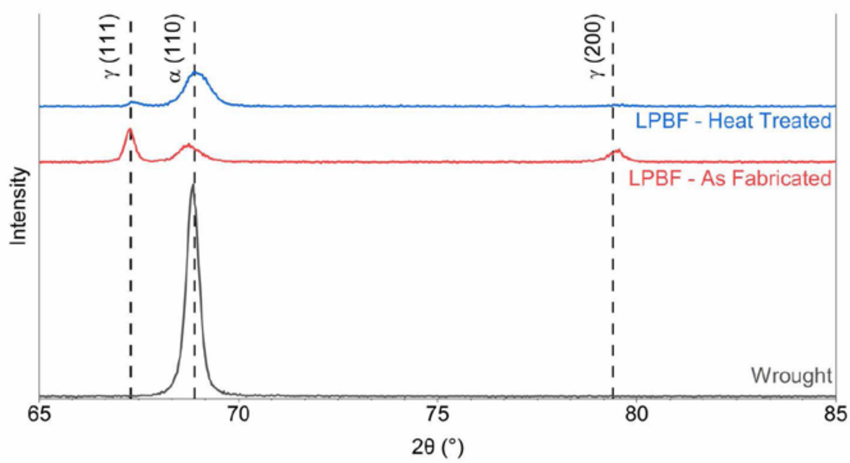

Figure 8—XRD patterns (Cr K-α radiation) for wrought 17-4PH and LPBF 17-4PH in the as-fabricated and heat-treated conditions.

General Discussion

As various AM methods will be applied to these powders, investigating the thermal response of the overspray powder is crucial for understanding the relationship between microstructure and properties. This investigation can provide insights into how different AM processes influence the microstructure and, consequently, the mechanical properties of the material. Furthermore, optimizing the microstructure and tailoring the properties can enable the customization of these materials for specific applications, enhancing their performance and suitability for a wide range of industrial uses.

Nitrogen can be picked up in both the feedstock powder and from the cover gas in part fabrication. Most conventional stainless steels have a low nitrogen content, so the impact of nitrogen in AM stainless steels must be addressed through in-situ techniques to develop a modified heat treatment.

Nitrogen has shown promise in being a viable alternative to interstitial carbon in gaseous treatment of steels. It demonstrates similar "case hardening" properties in steels and can be especially beneficial in stainless steels. However, using too much nitrogen can come at a cost, since austenite stabilization may not be desired. It is for this reason that optimization of microstructure is necessary, where in-situ techniques may be implemented. By using controlled heat-treatment tracking methods, lab scale iterations can be completed, assisting in the specific tailoring of microstructures. This information can be used and adopted on a wider scale in industrial processes to increase the properties and performance of materials.

Conclusion

- Three different martensitic and interstitially alloyed materials systems were investigated using the in-situ techniques: dilatometry, calorimetry, and thermogravimetry. These analytical techniques provide critical insights into the structural and thermal behavior of the material, enabling a comprehensive understanding of how the microstructure evolves under different thermal conditions. This is essential for optimizing processing parameters and tailoring the material properties for specific applications.
- The in-situ transformation behavior of high-carbon steel overspray powders was investigated using calorimetry. The decomposition of austenite, austenitization temperature and martensite formation could be recorded.
- In-situ thermogravimetric methods can track gaseous uptake or release during heat treatment, which remains an important topic with interstitial hardening of martensitic steels.
- In the case of 420 stainless steel, both grain structure and phase constituents varied as a function of nitrogen gradient through the sample. In particular, the martensite morphology demonstrated variation based on local nitrogen content.
- 17-4PH produced through LPBF in N_2 cover gas and nitrogen gas-atomized powder will maintain a primarily austenitic microstructure, despite having a lower nitrogen content than the nitrogen-loaded wrought 17-4PH, which still displayed a martensite transformation. This may be due to additional microstructural differences in the as-fabricated condition.
- Excess nitrogen has a significant impact on the martensite start temperature of stainless steels and promotes retained austenite in the final microstructure. As shown through dilatometry and microstructural analysis, an increased nitrogen content results in a suppressed M_s temperature.

Acknowledgements

We would like to express our gratitude to Asgaard Metals for their invaluable support in providing high-carbon steel for our research.

Qianchen Zeng is a Ph.D. student in the manufacturing program at Worcester Polytechnic Institute in the Department of Mechanical and Materials Engineering working on additive manufacturing and microstructure optimization of steel alloys powders.

Ellen Troyanosky is a Ph.D. candidate in the Center for Heat Treating Excellence at Worcester Polytechnic Institute. They started at WPI after receiving their B.S. in Materials Science and Engineering from the University of Pittsburgh in 2022. Their research focuses on the heat treatment and processing of steel.

Noah Kantor is a Ph.D. candidate at Worcester Polytechnic Institute studying Materials Science and Engineering and a research assistant for the Center for Heat Treating Excellence (CHTE), where his work pertains to quenching materials. He holds a B.S. in Chemical Engineering and an M.S. in Materials Science and Engineering.

Jianyu Liang is a professor of Mechanical and Materials Engineering at Worcester Polytechnic Institute, where she also holds affiliated appointments in Civil and Environmental Engineering and Chemical Engineering. She served at the Army Research Laboratories from 2013–2014 and Brown University in 2023–2024.

Thomas L. Christiansen is a professor at Worcester Polytechnic Institute in the Department of Mechanical and Materials Engineering. He is also the director of the Center for Heat Treating Excellence (CHTE), an industry-academia alliance that conducts research and development for the thermal processing industry.

References

1. P. Bajaj, A. Hariharan, A. Kini, P. Kürnsteiner, D. Raabe, and E. A. Jägle, "Steels in additive manufacturing: A review of their microstructure and properties," *Mater. Sci. Eng. A;* Vol. 772, p. 138633, 2020, doi: *https://doi.org/10.1016/j.msea.2019.138633*
2. G. B. Bang et al., "Microstructural and mechanical properties of AISI 440C stainless steel fabricated using selective laser melting," *Mater. Sci. Eng. A;* Vol. 860, p. 144259, Dec. 2022, *https://doi: 10.1016/j.msea.2022.144259*
3. V. M. Rodríguez, V. H. López-Morelos, V. K. Nadimpalli, D. Bue Pedersen, A. Ruiz, and M. A. J. Somers, "Effect of Heat Treatment Processes on the Microstructure and Mechanical Properties of Spray-Formed 440C Martensitic Stainless Steel," *Steel Res. Int.;* Vol. 94, No. 6, Jun. 2023.
4. S. H. Mohamed Salleh, M. Z. Omar, and S. Junaidi, "Phase Transformation and Thermal Analysis of Martensitic Stainless Steel 440C".
5. J. S. Park, J. H. Park, M.-G. Lee, J. H. Sung, K. J. Cha, and D. H. Kim, "Effect of Energy Input on the Characteristic of AISI H13 and D2 Tool Steels Deposited by a Directed Energy Deposition Process," *Metall. Mater. Trans. A;* Vol. 47, No. 5, pp. 2529–2535, May 2016, *https://doi: 10.1007/s11661-016-3427-5*
6. G. Zhang, H. Yuan, D. Jiao, Z. Li, Y. Zhang, and Z. Liu, "Microstructure evolution and mechanical properties of T15 high speed steel prepared by twin-atomiser spray forming and thermo-mechanical processing," *Mater. Sci. Eng. A;* Vol. 558, pp. 566–571, Dec. 2012, *doi: 10.1016/j.msea.2012.08.050.*
7. M. A. S. bin A. Rahim, M. bin Minhat, N. I. S. B. Hussein, and M. S. bin Salleh, "A comprehensive review on cold work of AISI D2 tool steel," *Metall. Res. Technol.;* Vol. 115, No. 1, Art. no. 1, 2018, *https://doi: 10.1051/metal/2017048*
8. F. Deirmina, N. Peghini, B. AlMangour, D. Grzesiak, and M. Pellizzari, "Heat treatment and properties of a hot work tool steel fabricated by additive manufacturing," *Mater. Sci. Eng. A,* Vol. 753, pp. 109–121, Apr. 2019, *https://doi: 10.1016/j.msea.2019.03.027*
9. F. Großwendt et al., "Additive manufacturing of a carbon-martensitic hot-work tool steel using a powder mixture – Microstructure, post-processing, mechanical properties," *Mater. Sci. Eng. A;* Vol. 827, p. 142038, Oct. 2021, *https://doi: 10.1016/j.msea.2021.142038*
10. W. Shan and Y. Lin, "T15 High Speed Steels Produced by High-Temperature Low-Pressure Short-Time Vacuum Hot-Pressing Combined with Subsequent Diffusion-Bonding Treatment," *Metals;* Vol. 13, No. 5, Art. no. 5, May 2023, *https://doi: 10.3390/met13050998*
11. H. Berns, R.L. Juse, J.W. Bouwman, B. Edenhofer, Solution Nitriding of Stainless Steels – "A New Thermochemical Heat Treatment Process*", T. Bell and K. Akamatsu, Eds., *Stainless Steel 2000: Thermochemical Surface Engineering of Stainless Steel.* London: CRC Press, 2020. *https://doi: 10.1201/9780367814151*
12. T. L. Christiansen, M. Villa, C. Tibollo, K. V. Dahl, and M. A. J. Somers, "High Temperature Solution Nitriding of Stainless Steels; Current Status and Future Trends," Vol. 75, No. 2, pp. 69–82, 2020, *https://doi: 10.3139/105.110406*
13. M. Pozuelo, J. E. Wittig, J. A. Jiménez, and G. Frommeyer, "Enhanced Mechanical Properties of a Novel High-Nitrogen Cr-Mn-Ni-Si Austenitic Stainless Steel via TWIP/TRIP Effects," *Metall. Mater. Trans. A;* Vol. 40, No. 8, pp. 1826–1834, Aug. 2009, *https://doi: 10.1007/s11661-009-9863-8*
14. N. Saenarjhan, J.-H. Kang, and S.-J. Kim, "Effects of carbon and nitrogen on austenite stability and tensile deformation behavior of 15Cr-15Mn-4Ni based austenitic stainless steels," *Mater. Sci. Eng. A;* Vol. 742, pp. 608–616, Jan. 2019, *https://doi: 10.1016/j.msea.2018.11.048*
15. H. W. Lee, J. H. Kong, D. J. Lee, H. Y. On, and J. H. Sung, "A study on high temperature gas nitriding and tempering heat treatment in 17Cr–1Ni–0.5C," *Mater. Des.;* Vol. 30, No. 5, pp. 1691–1696, May 2009, *https://doi: 10.1016/j.matdes.2008.07.023*
16. ASTM, "A564," ASTM International, West Conshohocken, PA, 2021.
17. E. A. Lass, M. R. Stoudt, and M. E. Williams, "Additively Manufactured Nitrogen-Atomized 17-4 PH Stainless Steel with Mechanical Properties Comparable to Wrought," *Metall. Mater. Trans. Phys. Metall. Mater. Sci.;* Vol. 50, No. 4, pp. 1619–1624, 2019.
18. R. Bhambroo, S. Roychowdhury, V. Kain, and V. S. Raja, "Effect of reverted austenite on mechanical properties of precipitation hardenable 17-4 stainless steel," *Mater. Sci. Eng. A;* Vol. 568, pp. 127–133, 2013, *https://doi: https://doi.org/10.1016/j.msea.2013.01.011*
19. M. Villa and M. A. J. Somers, "Cryogenic treatment of an AISI D2 steel: The role of isothermal martensite formation and 'martensite conditioning,'" *Cryog. Guildf.;* Vol. 110, p. 103131, 2020, *https://doi: 10.1016/j.cryogenics.2020.103131*
20. D. A. Porter, K. E. Easterling, and M. Y. Sherif, *Phase Transformations in Metals and Alloys,* 4th ed. CRC Press, 2022.
21. M. Umemoto, E. Yoshitake, and I. Tamura, "The morphology of martensite in Fe-C, Fe-Ni-C and Fe-Cr-C alloys," *J. Mater. Sci.;* Vol. 18, No. 10, pp. 2893–2904, Oct. 1983, *https://doi: 10.1007/BF00700770*
22. G. Krauss, "Martensite in steel: strength and structure," *Mater. Sci. Eng. A;* vol. 273–275, pp. 40–57, Dec. 1999, *https://doi: 10.1016/S0921-5093(99)00288-9*
23. L. D. Barlow and M. Du Toit, "Effect of Austenitizing Heat Treatment on the Microstructure and Hardness of Martensitic Stainless Steel AISI 420," *J. Mater. Eng. Perform.;* Vol. 21, No. 7, pp. 1327–1336, Jul. 2012, *https://doi: 10.1007/s11665-011-0043-9*
24. S. Cheruvathur, E. A. Lass, and C. E. Campbell, "Additive Manufacturing of 17-4 PH Stainless Steel: Post-processing Heat Treatment to Achieve Uniform Reproducible Microstructure," *JOM;* Vol. 68, No. 3, pp. 930–942, Mar. 2016, *https://doi: 10.1007/s11837-015-1754-4*

Decarbonization of the Iron and Steel Sector: Challenges and Opportunities

Samuel Henry, Nicholas Schneider, Sydney Hughes, Alexander Zoelle, Eric Grol, Timothy Fout, Sally Homsy

With government mandates to reduce greenhouse gas (GHG) emissions, decarbonizing the largest industrial emitters has become an essential research focus. The Environmental Protection Agency (EPA) reported that industrial point sources in the United States (U.S.) emitted 1.45 billion tons of carbon dioxide (CO_2) in 2022, accounting for 23 percent of all domestic CO_2 emissions for that year (Refs. 1,2). One of the largest contributors to industrial emissions is the iron and steel industry, which was responsible for 2.5 percent of total U.S. GHG emissions in 2023 (Ref. 3). Due to the large quantity of emissions available for capture from this industrial sector, iron/steel production facilities present an impactful opportunity for industrial decarbonization.

Various CO_2 capture technologies can be deployed in the iron/steel industry, including post-combustion capture with chemical solvents or membranes, precombustion capture with chemical solvents or membranes, and capture via calcium looping. There exist various examples of efforts to advance the decarbonization of iron/steel plants. The only operating, commercial-scale CO_2 capture plant in the iron/steel industry is the Al Reyadah facility in the United Arab Emirates (Ref. 4). This plant, commissioned in 2016, was initiated as a joint venture between Abu Dhabi National Oil Company (ADNOC) and Masdar, and captures CO_2 from a direct reduced iron (DRI)-based steel plant (Ref. 4). The capture plant has a nominal capacity of 800,000 tons of CO_2 per year and ADNOC asserted in 2023 that the plant enabled capture of 45 percent of emissions from DRI production (Ref. 4). The approximately 89 percent pure CO_2 product is dehydrated and used for enhanced oil recovery (EOR) in ADNOC's onshore oil fields (Ref. 4). In the U.S., the U.S. Department of Energy (DOE) has sponsored front end engineering design (FEED) studies, pre-FEED studies, and pilot demonstrations examining the addition of capture to iron and steel plants. This includes a pre-FEED study led by Dastur International Inc. in coordination with Cleveland-Cliffs Inc. assessing the implementation of ION Energy's solvent-based, post-combustion capture technology to capture 95 percent of CO_2 from blast furnace (BF) flue gas from a steel plant located in Burns Harbor, IN, producing 5 million (M) tons of steel per year. A DOE-sponsored FEED study led by The University of Illinois, in partnership with Air Liquide, Visage Energy Corporation, Hatch Associates Consultants Inc., Midrex Technologies Inc., ArcelorMittal, and voestalpine Texas LLC, is examining the use of Air Liquide's Cryocap technology to capture 95 percent of the total CO_2 emissions from a Texas hot briquetted iron plant.

In 2023, the National Energy Technology Laboratory (NETL) released its report, "Cost of Capturing CO_2 from Industrial Sources," (Industrial Sources Report) intending to estimate the levelized cost of CO_2 captured (LCOC) from selected industrial processes including iron/steel facilities (Ref. 5). A traditional pathway to produce steel from iron ore comprising a BF integrated with a basic oxygen furnace (BOF), also referred to as an integrated steel mill, is considered for this analysis. While integrated steel mills have multiple CO_2 emissions sources, this work focuses on applying capture to the three largest and highest concentration sources. The capture system utilized is the CANSOLV CO_2 capture technology commercially offered by Shell. CANSOLV is an amine-based, acid gas removal (AGR) process designed to recover high purity CO_2 from dilute flue gas streams and is assessed at capture rates of both 90 and 99 percent. The LCOC for this system is estimated using the methodology established in NETL's Quality Guidelines for Energy System Studies (QGESS) document, "Cost Estimation Methodology for NETL Assessments of Power Plant Performance" (Ref. 6). NETL's 2023 Industrial Sources Report presents the LCOC in December 2018 dollars.

The current paper leverages the Industrial Sources Report's iron/steel cases, expands the discussion, and provides the LCOC in January 2024 dollars. The financial assumptions are updated with input from NETL's Energy Markets Analysis Team and are based on 2024 iron/steel industrial sector market data.

This paper was first presented at the 17th International Conference on Greenhouse Gas Control Technologies, GHGT-17, 20th–24th October 2024 Calgary, Canada. Available at SSRN: ssrn.com/abstract=5070025 or dx.doi.org/10.2139/ssrn.5070025

Background

Iron/Steel Production Methods

There are two commercial methods of iron production in operation today: the blast furnace (BF) method and direct reduced iron (DRI) method. In the BF method, coke and sintered iron are fed to the top of the BF while hot blast gas is fed through the side. Coke is oxidized to form CO_2 which subsequently reacts with more coke to produce carbon monoxide (CO). This CO facilitates the reduction of iron oxides to form pig iron, a high carbon iron alloy. In 2023, the U.S. produced 20.6 M tons of pig iron and imported an additional 4.4 M tons (Ref. 7). The DRI method is a newer alternative iron production pathway. DRI is made by reducing iron ore with gas, eliminating some pre-processing steps required for BF operation (Ref. 8). Typical reductants used to make DRI are coal syngas, natural gas, or hydrogen (H_2) depending on availability. In 2023, DRI production constituted 5.2 M tons of iron production in the U.S. (Ref. 7).

Steel is produced by reducing the carbon content of iron in a furnace, of which there are two types in commercial operation. Traditionally, a BOF is used to remove carbon by blowing hot oxygen through molten pig iron. A newer alternative is the electric arc furnace (EAF), which uses electricity to melt scraps and recycled steel to form a steel product. While scrap and recycled steel is considered the main feed for EAF mills, some have been configured to use feeds of pig iron or DRI (Ref. 8). As of 2023, 31.7 percent of U.S. steel was produced via EAFs, with the remainder produced via BOFs (Ref. 7).

The traditional pathway to produce steel from the starting raw material, iron ore, is a BF integrated with a BOF, also referred to as an integrated steel mill. For these facilities, approximately 69 percent of emissions are present in the BF gas, which is often used as a heat source or a low-grade fuel for an integrated power plant (Ref. 9). Consequently, there are many different point sources for potential carbon capture in an integrated steel mill resulting in a complex challenge for decarbonization efforts. Researchers have investigated capturing CO_2 from coke ovens, hot stoves, power plant stacks (PPS), and lime kiln emissions to avoid impacting the BF gas and its benefits to the plant (Ref. 10). Furthermore, much research has focused on decarbonizing BF gas without directly treating it in a CO_2 capture plant. Replacing coke with biomass is one option, but only 10 percent of coke can feasibly be replaced due to an unsustainable drop in coke strength with higher replacement (Ref. 8). Another approach involves the use of H_2 as an additional reducing agent to reduce the amount of coke required. One study looked at using electrolysis-derived H_2 as an auxiliary reductant and found that emissions could be reduced by 21.4 percent under optimized conditions (Ref. 11). Due to its widespread commercial usage, the BF-BOF pathway was chosen for analysis in this study.

Another steel production pathway is the mini mill, in which a sole EAF is fed scrap and recycled steel (Ref. 9). Mini mills emit approximately 0.6 to 0.9 tons of CO_2 per ton of steel (tons CO_2/ton steel), representing a significant reduction compared to 2.2 tons CO_2/ton steel for integrated steel mills (Ref. 9). However, this reduction is due to the use of scrap and recycled steel which are not available in sufficient quantities to satisfy the entire U.S. steel demand.

A new, alternative pathway being explored is the combination of DRI production with an EAF (Refs. 8,12). In a study from Argonne National Laboratory, a DRI-EAF pathway with no scrap steel feed using grid electricity and natural gas reductant showed a 14.3 percent drop in emissions and an 8.9 percent lower cost compared to BF-BOF steel (Ref. 8). The same configuration with a reductant comprising 83 percent renewable H_2 and 17 percent natural gas showed a 46.6 percent reduction in CO_2 emissions and a 6.6 percent greater cost as compared to BF-BOF steel (Ref. 8). Other ways to reduce emissions through the DRI pathway involve using renewable natural gas or low-carbon electricity, but these options will incur additional costs.

Size Range

According to the World Steel Association, the U.S. accounted for approximately 81.4 M tons of steel production in 2023. Of these 81.4 M tons of steel, 31.7 percent was produced using an EAF and the balance using the more traditional BOF (Ref. 7). The resulting steel product from an EAF process contains approximately 100 percent recycled steel, whereas the BOF product contains 25 percent recycled steel on average (Ref. 7). The utilization of scrap steel results in lower CO_2 emissions for an EAF process (0.6–0.9 tons CO_2/ton steel) versus the BOF process (2.2 tons CO_2/ton steel) (Ref. 9). The combination of generally smaller EAF plants and lower concentration of EAF plant CO_2 emissions projects to a higher LCOC from an EAF process. Therefore, this study focuses on CO_2 capture from BOF process steel plants. Furthermore, as no new BOF steel plants are expected to be constructed in the U.S. in the near term, only retrofit application of CO_2 capture is considered. The total production capacity, as given by the World Steel Association for BOF plants in the United States in 2023, was 55.6 M tons (Ref. 7).

Methodology

CO_2 Point Sources

A study by Wiley, et al., published in 2010, assessed the opportunities for CO_2 capture in Australian iron and steel mills (Ref. 9). This study utilized stream data from an Australian BOF steel mill, and within the base plant, the largest source of CO_2 comes from the top gas of the BF as is typical in an integrated steel mill; however, this stream is not directly vented. Instead, the BF gas is cleaned and used in the plant as low-grade fuel, and rather than having a high-content CO_2 point source from the blast furnace gas, the CO_2 is distributed throughout the plant as smaller CO_2 point sources. The resulting CO_2 point sources available to be captured include the PPS, coke oven gas (COG), BF stove (BFS), sinter stack, blown oxygen steelmaking stack, hot strip mill stack, plate mill stack, and lime kiln, based on the configuration detailed by Wiley, et al. (Ref. 9). The three highest CO_2 concentrations of these point sources are the COG at 27 volume percent, the BFS at 21 volume percent, and the PPS at 23 volume percent. These three point sources are evaluated in this analysis, and their characteristics are described in Table 1.

Personal communication with a former U.S. Steel Braddock, PA, facility employee indicated that while the coke ovens are approximately five miles from the BF, the COG is circulated back to the BF to preheat the incoming air. Therefore, these two streams are located relatively close to one another and may be combined. As such, this analysis assumes two CO_2 capture units with two corresponding compression trains. Figure 1 is a simplified block flow diagram (BFD) of the Braddock steel mill.

Design Input and Assumptions

The following is a list of design inputs and assumptions specific to the iron/steel process that were made for the purpose of this study:

- The representative BOF integrated steel mill has a production capacity of 2.54 M tonnes/year.
- The CO_2 generated is 3,738,928 tons CO_2/year at 100 percent capacity factor (CF).
- There are three high purity sources: COG, BFS, and COG PPS. The COG and BFS are combined into one stream due to plot plan and total 1,864,388 tons CO_2/year (at 100 percent CF); COG PPS utilizes its own separation and compression facility and generates 1,874,540 tons CO_2/year (at 100 percent CF).
- Since there are two separate capture systems, 4.6 operators are considered (i.e., 2.3 operators per capture system).
- As a low purity source, separation, compression, and cooling are required. Separation is accomplished using Shell's CANSOLV solvent-based CO_2 capture system.
- CO_2 capture rates of 90 and 99 percent are evaluated.
- The CO_2 quality is based on the EOR pipeline standard as mentioned in NETL's QGESS for CO_2 Impurity Design Parameters (Ref. 13).

CO_2 Capture System

The AGR system utilized is the CANSOLV CO_2 capture technology commercially offered by Shell. This amine-based, post-combustion process is designed to recover high purity CO_2 from dilute streams that contain O_2, such as flue gas from coal-fired power plants, combustion turbine exhaust gas, and other industrial waste streams. The AGR unit also provides polishing of residual sulfur components in the CO_2 capture stream. A dedicated natural gas-fired boiler is also included to generate the steam required for the capture system, but the flue gas from the boiler is not routed to the CO_2 capture system. The performance and cost information for the AGR units employed herein are based on data provided by Shell in 2021. The CO_2 removal efficiency of the AGR unit is represented at two rates, 90 and 99 percent for each case. A typical flowsheet for the process is shown in Figure 2.

Description	PPS	COG	BFS
CO_2 Emitted/Tonne Steel produced	0.74	0.35	0.39
Pressure (psia)	14.7	14.7	14.7
Temperature (°F)	572	212	572
Composition (vol %)			
Nitrogen (N_2)	67.0	67.0	68.0
Water (H_2O)	8.0	5.0	10.0
CO_2	23.0	27.0	21.0
O_2	1.0	1.0	1.0

Table 1—BOF iron and steel plant characteristics (Ref. 9).

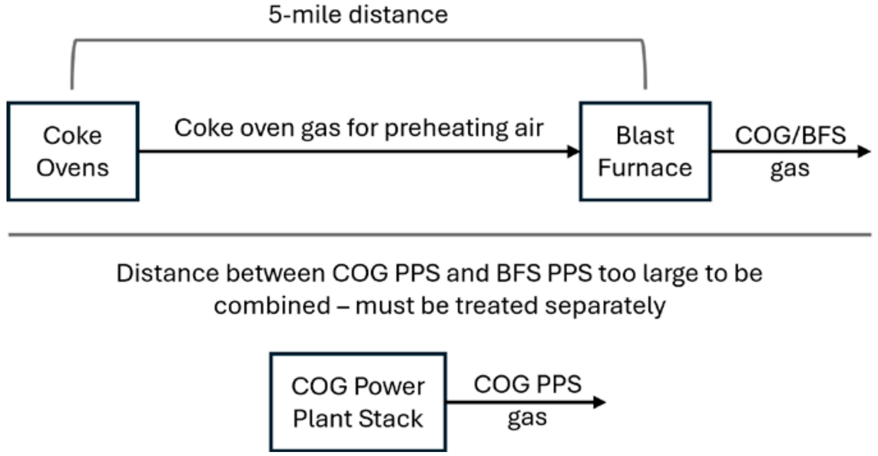

Figure 1—Braddock steel mill plot plan.

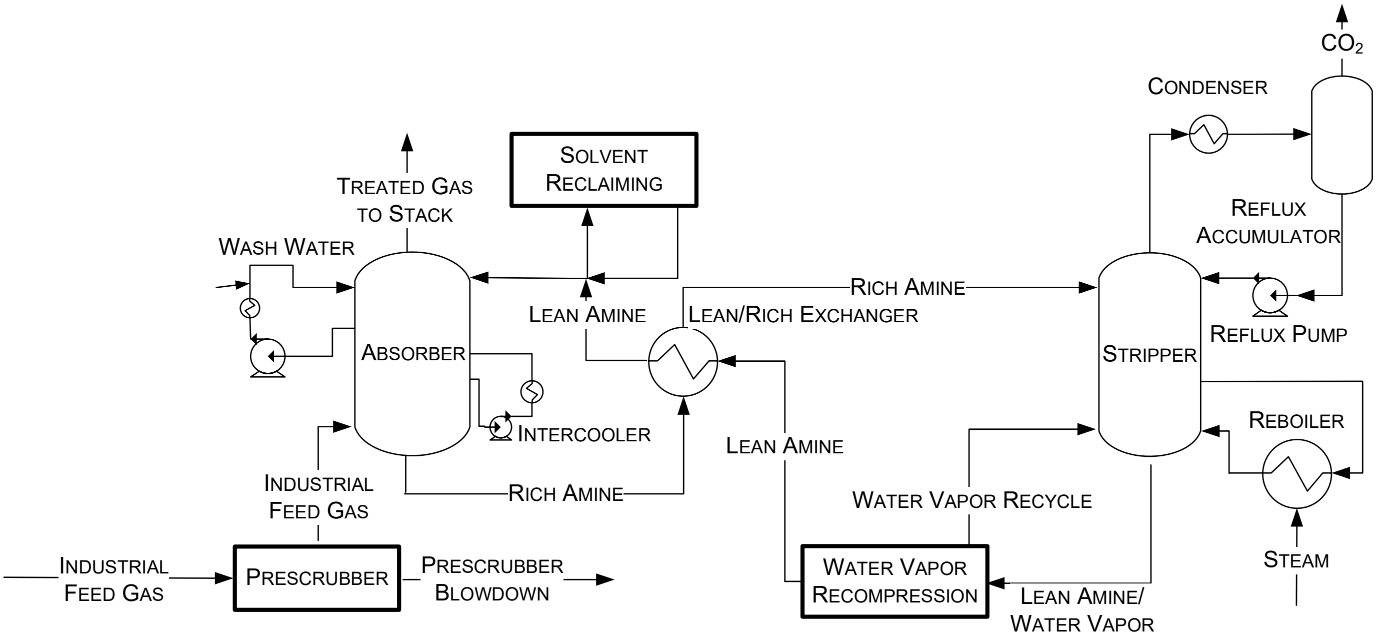

Figure 2—Shell's CANSOLV CO_2 capture system typical process flow diagram.

Centrifugal Compressor

Compression of the CO_2 product is required for pipeline transportation and storage or use. As such, integrally geared centrifugal compression trains (8 stages each) are included with each CO_2 product stream. All compressors discharge at a pressure of 2,214.7 psia (2,200 psig). This is the pipeline pressure specification as stated in NETL's QGESS for CO_2 Impurity Design Parameters (Ref. 13). However, it should be noted that pressure requirements can vary by location, and pressures as low as 1,200 may be acceptable (Ref. 14). A quote provided for the development of NETL's "Cost and Performance Baseline for Fossil Energy Plants Volume 1: Bituminous Coal and Natural Gas to Electricity," Revision 4, was utilized to represent the cost for this equipment (Ref. 15).

Cost Estimation Methodology and Financial Assumptions

To the extent possible, cost results for this analysis are estimated using the methodology established in NETL's Quality Guidelines for Energy System Studies (QGESS) document, "Cost Estimation Methodology for NETL Assessments of Power Plant Performance" (Ref. 6). Detailed information about topics such as contracting strategy; engineering, procurement, and construction (EPC) contractor services; estimation of capital cost contingencies; owner's costs; cost estimate scope; economic assumptions; and finance structures are available in this document. The financial assumptions employed were developed by NETL's Energy Markets Analysis Team in 2024 based on market data reflective of the iron/steel industrial sector.

Levelized Cost of CO_2 Captured

The LCOC as defined by Equation 1, considers the equipment required for CO_2 removal and compression, as well as the balance of plant equipment, operation and maintenance, purchased power, and fuel costs:

$$LCOC\left(\frac{\$}{tonne\ CO_2}\right) = \frac{TOC * CCF + FOM + VOM + PSG}{CF * tonnes\ CO_2\ captured\ per\ year} \tag{1}$$

Where TOC is the total overnight costs of CO_2 capture equipment, CCF is the capital charge factor, FOM is the annual fixed operation and maintenance (O&M) costs, VOM—is the annual variable O&M costs, PSG is power and steam generation (natural gas purchase) costs, and CF is the capacity factor (85 percent assumed).

Results and Discussion

Block Flow Diagrams and Stream Tables

For the COG/BFS case, the COG stream and BFS stream are mixed and sent to the CO_2 capture system. Water and solids recovered from the capture system are sent to waste treatment. The CO_2 stream is then compressed with interstage cooling and after-cooled before reaching the EOR pipeline. Figure 3 shows the BFD for this process, and Table 2 and Table 3 show the stream table for this process with 99 percent and 90 percent capture, respectively.

In the same manner, the COG PPS stream is sent to the CANSOLV CO_2 capture system. Water and solids recovered from the capture process are sent to waste treatment. The CO_2 stream is then compressed with interstage cooling and after-cooled before reaching the EOR pipeline. Figure 4 shows the BFD for this process, and Table 4 and Table 5 show the stream table for this process with 99 percent and 90 percent capture, respectively.

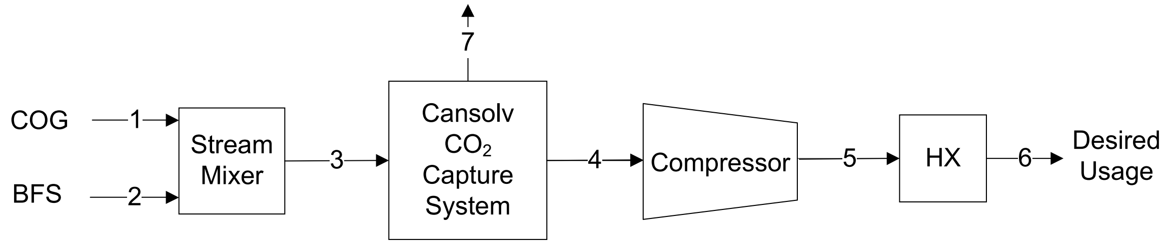

Figure 3—CO_2 capture BFD for COG/BFS.

	1	2	3	4	5	6	7
V-L Mole Fraction							
CO_2	0.2700	0.2100	0.2345	0.9879	0.9995	0.9995	0.0034
H_2O	0.0500	0.1000	0.0795	0.0121	0.0005	0.0005	0.0237
N_2	0.6700	0.6800	0.6759	0.0000	0.0000	0.0000	0.9588
O_2	0.0100	0.0100	0.0100	0.0000	0.0000	0.0000	0.0141
Total	1.0000	1.0000	1.0000	1.0000	1.0000	1.0000	1.0000
V-L Flowrate (kg_{mol}/hr)	8,443	12,173	20,616	4,845	4,788	4,788	14,533
V-L Flowrate (kg/hr)	269,106	370,224	639,331	211,692	210,637	210,637	405,309
Temperature (°C)	100	300	219	31	80	30	38
Pressure (MPa, abs)	0.10	0.1	0.1	0.2	15.3	15.3	0.1
Steam Table Enthalpy (kJ/kg)	3,700	3,593	3,638	8,793	8,758	8,755	309.0
Aspen Plus Enthalpy (kJ/kg)	-3,638	-3,217	-3,394	-8,961	-9,042	-9,195	-240.1
Density (kg/m^3)	1.0	0.6	0.8	3.5	432.5	630.1	1.1
V-L Molecular Weight	31.9	30.4	31.0	43.7	44.0	44.0	27.9

Table 2—Iron/steel COG/BFS stream table with 99 percent capture.

	1	2	3	4	5	6	7
V-L Mole Fraction							
CO_2	0.2700	0.2100	0.2346	0.9881	0.9995	0.9995	0.0322
H_2O	0.0500	0.1000	0.0795	0.0119	0.0005	0.0005	0.0237
N_2	0.6700	0.6800	0.6759	0.0000	0.0000	0.0000	0.9303
O_2	0.0100	0.0100	0.0100	0.0000	0.0000	0.0000	0.0137
Total	1.0000	1.0000	1.0000	1.0000	1.0000	1.0000	1.0000
V-L Flowrate (kg_{mol}/hr)	8,443	12,173	20,616	4,405	4,354	4,354	14,978
V-L Flowrate (kg/hr)	269,106	370,224	639,331	192,516	191,573	191,573	424,582
Temperature (°C)	100	300	219	31	80	30	38
Pressure (MPa, abs)	0.10	0.1	0.1	0.2	15.3	15.3	0.1
Steam Table Enthalpy (kJ/kg)	3,700	3,593	3,638	8,793	8,758	8,755	691.0
Aspen Plus Enthalpy (kJ/kg)	-3,638	-3,217	-3,394	-8,960	-9,042	-9,195	-636.8
Density (kg/m^3)	1.0	0.6	0.8	3.5	432.5	630.1	1.1
V-L Molecular Weight	31.9	30.4	31.0	43.7	44.0	44.0	28.3

Table 3—Iron/steel COG/BFS stream table with 90 percent capture.

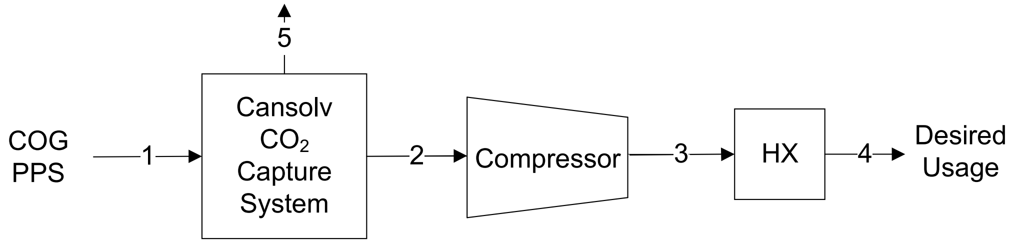

Figure 4—CO_2 capture BFD for COG PPS.

	1	2	3	4	5
V-L Mole Fraction					
CO_2	0.2700	0.2100	0.2345	0.9879	0.9995
H_2O	0.0500	0.1000	0.0795	0.0121	0.0005
N_2	0.6700	0.6800	0.6759	0.0000	0.0000
O_2	0.0100	0.0100	0.0100	0.0000	0.0000
Total	1.0000	1.0000	1.0000	1.0000	1.0000
V-L Flowrate ($_{kgmol}$/hr)	8,443	12,173	20,616	4,845	4,788
V-L Flowrate (kg/hr)	269,106	370,224	639,331	211,692	210,637
Temperature (°C)	100	300	219	31	80
Pressure (MPa, abs)	0.10	0.1	0.1	0.2	15.3
Steam Table Enthalpy (kJ/kg)	3,700	3,593	3,638	8,793	8,758
Aspen Plus Enthalpy (kJ/kg)	-3,638	-3,217	-3,394	-8,961	-9,042
Density (kg/m^3)	1.0	0.6	0.8	3.5	432.5
V-L Molecular Weight	31.9	30.4	31.0	43.7	44.0

Table 4—Iron/steel COG PPS stream table with 99 percent capture.

	1	2	3	4	5
V-L Mole Fraction					
CO_2	0.2700	0.2100	0.2345	0.9879	0.9995
H_2O	0.0500	0.1000	0.0795	0.0121	0.0005
N_2	0.6700	0.6800	0.6759	0.0000	0.0000
O_2	0.0100	0.0100	0.0100	0.0000	0.0000
Total	1.0000	1.0000	1.0000	1.0000	1.0000
V-L Flowrate (kg_{mol}/hr)	8,443	12,173	20,616	4,845	4,788
V-L Flowrate (kg/hr)	269,106	370,224	639,331	211,692	210,637
Temperature (°C)	100	300	219	31	80
Pressure (MPa, abs)	0.10	0.1	0.1	0.2	15.3
Steam Table Enthalpy (kJ/kg)	3,700	3,593	3,638	8,793	8,758
Aspen Plus Enthalpy (kJ/kg)	-3,638	-3,217	-3,394	-8,961	-9,042
Density (kg/m^3)	1.0	0.6	0.8	3.5	432.5
V-L Molecular Weight	31.9	30.4	31.0	43.7	44.0

Table 5—Iron/steel COG PPS stream table with 90 percent capture.

Performance Summary

The performance summary for both 90 and 99 percent capture cases in the COG/BFS section of the steel mill is provided in Table 6, while that of the COG PPS section is shown in Table 7.

Cost Results

The cost results for CO_2 capture retrofit in an integrated steel mill are presented in this section. The LCOC for the total capture system at both 99 and 90 percent capture in January 2024 real dollars is presented in Figure 5. LCOC is broken down into its components: capital, fixed O&M, variable O&M, and purchased power and fuel. Figure 6 presents the sensitivity of LCOC to steel plant scale. For comparison, Figure 7 provides insight into the decarbonization potential of applying capture to different industries and the cost associated with the different applications.

Item	2.54 M tonne steel/year with 90 percent CO_2 capture (kWe)	2.54 M tonne steel/year with 99 percent CO_2 capture (kWe)
CO_2 Capture Auxiliaries	4,800	5,400
Steam Boiler Auxiliaries	510	560
CO_2 Compressor	14,660	16,120
Circulating Water Pumps	1,480	1,610
Cooling Tower Fans	770	830
Total Auxiliary Load	22,220	24,520

Table 6—Performance summary for iron/steel COG/BFS section.

Item	2.54 M tonne steel/year with 90 percent CO_2 capture (kWe)	2.54 M tonne steel/year with 99 percent CO_2 capture (kWe)
CO_2 Capture Auxiliaries	4,900	5,400
Steam Boiler Auxiliaries	520	570
CO_2 Compressor	14,750	16,210
Circulating Water Pumps	1,490	1,620
Cooling Tower Fans	770	830
Total Auxiliary Load	22,430	24,630

Table 7—Performance summary for iron/steel COG PPS section.

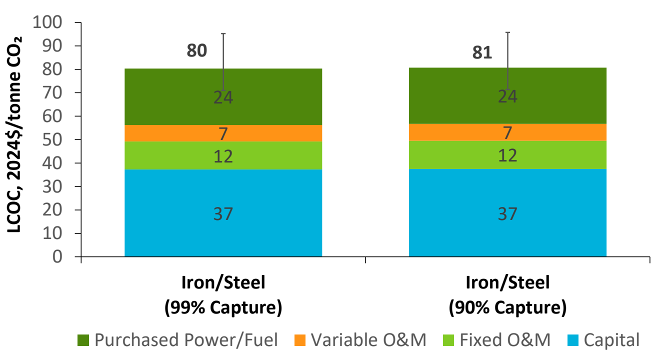

Figure 5—LCOC for 2.54 M tons/year iron/steel retrofit cases.

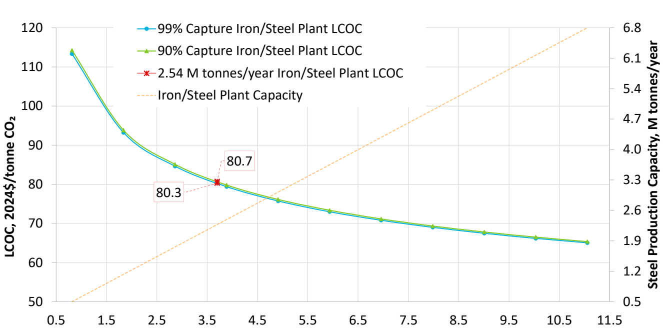

Figure 6—LCOC sensitivity to iron/steel retrofit scale.

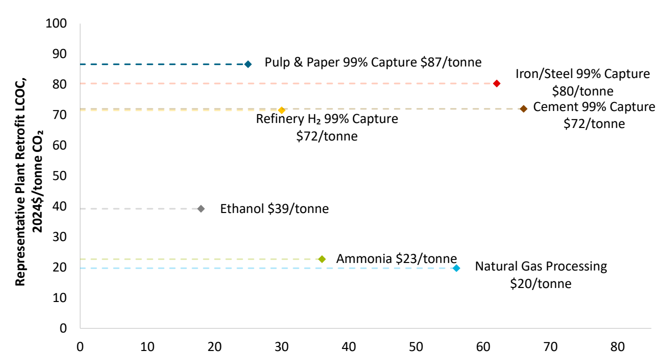

Figure 7—LCOC and decarbonization potential of applying capture at different industrial applications.

Conclusions

Two CO_2 capture and compression systems for a 2.54 M tons/year integrated steel mill were modeled to estimate the LCOC from the COG and BFS combined flue gas stream and from the COG PPS exhaust. The results showed the LCOC of CO_2 to be \$80.3/ton CO_2 and \$80.7/ton CO_2 for a retrofit site with 99 and 90 percent capture, respectively. While the LCOC for retrofitting iron/steel mills is higher compared to other point sources evaluated in the Industrial Sources Report, mainly due to the relatively lower purity CO_2 available, the quantity of CO_2 to be captured from such a process makes adding capture to iron/steel plants attractive as it would represent a significant GHG reduction.

Acknowledgements

This work was funded by the U.S. Department of Energy's Office Fossil Energy and Carbon Management through National Energy Technology Laboratory's ongoing research under the Point Source Capture Multi Year Research Plan.

Disclaimer

This project was funded by the United States Department of Energy, National Energy Technology Laboratory an agency of the United States Government, through a support contract. Neither the United States Government nor any agency thereof, nor any of its employees, nor the support contractor, nor any of their employees, makes any warranty, express or implied, or assumes any legal liability or responsibility for the accuracy, completeness, or usefulness of any information, apparatus, product, or process disclosed, or represents that its use would not infringe privately owned rights. Reference herein to any specific commercial product, process, or service by trade name, trademark, manufacturer, or otherwise does not necessarily constitute or imply its endorsement, recommendation, or favoring by the United States Government or any agency thereof. The views and opinions of authors expressed herein do not necessarily state or reflect those of the United States Government or any agency thereof.

This article is authored by federal staff and site support contractors at the Department of Energy Office of Fossil Energy and Carbon Management's National Energy Technology Laboratory (NETL). The authors use their techno-economic analysis expertise for evaluating technologies and identifying opportunities in support of economic viability and energy security.

Samuel Henry

Nicholas Schneider

Sydney Hughes

Alexander Zoelle

Eric Grol

Timothy Fout

Sally Homsy

References

1. EPA, "Greenhouse Gas Inventory Data Explorer," 2023. [Online]. Available: *https://cfpub.epa.gov/ghgdata/inventoryexplorer/* [Accessed 9 December 2024].
2. EPA, "Sources of Greenhouse Gas Emissions," 2019. [Online]. Available: *https://www.epa.gov/ghgemissions/sources-greenhouse-gas-emissions* [Accessed 19 September 2024].
3. EPA, "Facility Level Information on Greenhouse Gases Tool," 2020. [Online]. Available: *https://ghgdata.epa.gov/ghgp/main.do?site_preference=normal* [Accessed 9 December 2024].
4. S. Nicholas and S. Basirat, "Carbon Capture for Steel?," Institute for Energy Economics and Financial Analysis, 2024.
5. NETL, "Cost of Capturing CO_2 from Industrial Sources," U.S. Department of Energy, Pittsburgh, 2023.
6. NETL, "Quality Guidelines for Energy System Studies: Cost Estimation Methodology for NETL Assessments of Power Plant Performance," U.S. Department of Energy, Pittsburgh, 2019.
7. World Steel Association, "World Steel in Figures," 2024. [Online]. Available: *https://worldsteel.org/data/world-steel-in-figures-2024/* [Accessed 19 November 2024].
8. G. Zang, P. Sun, A. Elgowainy, P. Bobba, C. McMillan, O. Ma, K. Podkaminer, N. Rustagi, M. Melaina and M. Koleva, "Cost and Life Cycle Analysis for Deep CO_2 Emissions Reduction for Steel Making: Direct Reduced Iron Technologies," *Steel Research International,* Vol. 94, No. 6, 2023.
9. D. Wiley, M. Ho and A. Bustamante, "Assessment of opportunities for CO_2 capture at iron and steel mills: An Australian perspective," *Energy Procedia,* Vol. 4, pp. 2654-2661, 2011.
10. J. Perpiñán, P. B. M. Begoña, V. Eveloy, P. Kanna, A. Raj, P. Lisbona and L. Romeo, "Integration of carbon capture technologies in blast furnace based steel making: A comprehensive and systematic review," *Fuel,* Vol. 336, 2023.
11. NETL, "Enabling Production of Low Carbon Emissions Steel through CO_2 Capture from Blast Furnace Gases," NETL, 2023. [Online]. Available: *https://www.netl.doe.gov/project-information?p=FE0031937* [Accessed 20 November 2024].
12. NETL, "Industrial Carbon Capture from an Existing Hot Briquetted Iron Manufacturing Facility using the Cryocap FG Technology," NETL, 2023. [Online]. Available: *https://www.netl.doe.gov/project-information?p=FE0032221* [Accessed 20 November 2024].
13. NETL, "Quality Guidelines for Energy System Studies: CO2 Impurity Design Parameters," DOE/NETL-PUB-22529, Pittsburgh, 2019.
14. NETL, "Carbon Dioxide Enhanced Oil Recovery: Untapped Domestic Energy Supply and Long Term Carbon Storage Solution," U.S. DOE/NETL, Pittsburgh, 2010.
15. NETL, "Cost and Performance Baseline for Fossil Energy Plants Volume 1: Bituminous Coal and Natural Gas to Electricity Revision 4," DOE, Pittsburgh, 2019.
16. AACE International, Cost Estimate Classification System—As Applied in Engineering, Procurement, and Construction for the Process Industries; TCM Framework 7.3—Cost Estimating and Budgeting, AACE International, 2005.

Gleason

CELEBRATES 160TH ANNIVERSARY

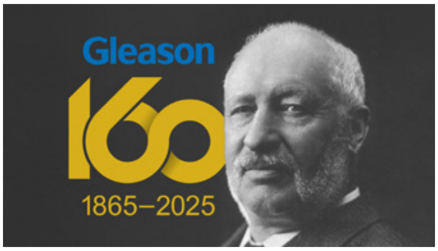

This year marks an important milestone as Gleason Corporation celebrates its 160th anniversary. Founded in 1865 by William Gleason, the company has transformed from a small workshop to a global leader in gear technology, offering comprehensive solutions that encompass design software, manufacturing and metrology equipment, tooling, aftermarket services, and an extensive training program.

Gleason's journey began with the invention of the first bevel gear planer in 1874, a pivotal development that significantly propelled the gear manufacturing industry forward. This innovation was the first of many that established Gleason as a pioneer in gear technology, contributing to many historical technology milestones, Gleason products helped shape the Panama Canal in 1903, invented the Spiral Bevel Gear in 1913, a few years later the hypoid gear, provided transmissions for the famed WWII Sherman tank, Curvic Couplings and critical geared components for the Apollo space missions, and the highly successful breakthrough technologies like the Phoenix and Genesis Machine Series.

Over the years, in addition to organic growth, Gleason has expanded its reach and capabilities through the strategic acquisitions of Hurth Maschinen und Werkzeuge in Munich, the Hermann Pfauter Group in Ludwigsburg, Germany, and adding metrology systems, automation solutions and plastic gears to its product range. These strategic additions have not only expanded its product offerings but also its geographical footprint, establishing manufacturing and service sites in major industrial hubs across the globe, including state-of-the-art factories built in Suzhou, China, and Bangalore, India. In 2017, Gleason acquired Swiss KISSsoft AG, integrating leading gear design and simulation software into its portfolio, becoming the first company in the industry to combine design, manufacturing and metrology elements across virtually all gear types into a Gear Technology Ecosystem.

"We are proud of our rich history and the groundbreaking innovations we have driven in the past 160 years," says John J. Perrotti, chairman and chief executive officer of Gleason Corporation. "Celebrating 160 years is not just about looking back with pride, but also about looking forward to continuing our commitment to excellence, customer focus, and technological leadership." Gleason continues to advance the industry with high-precision, innovative solutions that meet and exceed the challenging demands of its customers worldwide.

gleason.com

Ipsen USA

ANNOUNCES MANAGEMENT CHANGES IN CUSTOMER SERVICE TEAM

Ipsen is pleased to announce the promotion of Evan Hundley to retrofits manager and the appointment of Lu Chouraki as field service manager.

Evan Hundley

Since joining Ipsen in October 2023 as a project manager in the retrofits department, Hundley has demonstrated strong leadership and a commitment to continuous improvement. With a degree in industrial engineering from Iowa State University, she has applied her expertise in lean manufacturing to drive process improvements, including a Kaizen event to optimize operations and Ipsen's ERP system. Hundley has also enhanced the project manager role by improving project organization, financial reporting, and cross-department collaboration. As retrofits manager, she will lead the retrofits team to improve response times, streamline pricing and proposals, and provide tailored solutions that extend equipment lifespan and efficiency, driving long-term customer satisfaction.

Lu Chouraki

Chouraki rejoined Ipsen in June 2022 as manager of business development and has been instrumental in launching Ipsen's HUB service model, expanding it across six U.S. regions. He first joined Ipsen in 2015 as a field service engineer before being promoted to regional service manager in 2018. His extensive experience within Ipsen's service operations, combined with his industry knowledge, makes him uniquely qualified to lead the field service team. As field service manager, Chouraki will oversee all regional service managers and field service engineers, focusing on streamlining processes, improving response times, and enhancing customer support. He will also drive the continued expansion of Ipsen's HUBs and develop his team into subject matter experts, supporting Ipsen's commitment to outstanding service delivery and customer satisfaction.

"We are excited for Evan and Lu to take on new roles. These two leaders have already made significant contributions to Ipsen's success," said John Dykstra, Ipsen's chief service officer. "Their experience and dedication to improving our operations and customer support will be key as we continue to innovate and enhance our service offerings."

Ipsen is confident that under Hundley and Chouraki's leadership, the company will continue to drive success and further enhance customer support and service operation.

ipsenglobal.com

AFC-Holcroft

ANNOUNCES COO RETIREMENT

Ron Waligora, chief operating officer for AFC-Holcroft has announced his retirement date of May 4, 2025.

Ron graduated with a BSME degree from Michigan Technological University and was immediately hired by Holcroft in the summer of 1988 as a field service engineer. Throughout his 36 years with the company, Waligora moved through the engineering disciplines and eventually into a management role as mechanical engineering manager and later senior engineer manager in 2015.

In the spring of 2023 Waligora and Tracy Dougherty assumed the roles of chief operating officers. This dual role of leadership allowed the company to operate smoothly with high standards of excellence. It was known in 2023 that upon Ron's retirement Tracy would assume the role of president and CEO. This will occur January 1, 2025, during the transition period.

The timing of Waligora's retirement coincides with his wife, Jill's, retirement and he has expectations of supporting AFC-Holcroft if and when necessary, while enjoying the next phase of his life.

In his company announcement Waligora pointed out this message to the team, "Trust each other. Always strive to be great, and if you're lucky like me, good things will continue to happen. This can only happen if you love your job. I certainly have."

afc-holcroft.com

ALD Vacuum Technologies

DEVELOPS PLANT CONCEPT FOR DAIDO STEEL

Daido Steel Co. Ltd. is making an important contribution to the development of tomorrow's society and is therefore increasing its production capacity for high-quality stainless-steel production at its Chita site in Japan. ALD Vacuum Technologies was tasked to develop a plant concept specifically tailored to the needs of Daido Steel so that the best materials for the semiconductor industry can be produced. The first plant was put into operation in December 2024 and the finished ingots are already being processed. With this new remelting plant, the international company is constantly developing to meet the strong demand for stainless steel and nickel alloys. The second plant will start operations in March 2025. Further plants are to be integrated into the new plant over the next few years.

VAR-remelted steel is very pure and has a homogeneous microstructure, so its properties are ideally suited to the highest demands. A high-quality and durable material is produced that greatly develops first-class industries in the semiconductor industry. ALD is pleased to be part of this success and we thank you for your cooperation on this pioneering project.

ald-vt.com

Liebherr

LAUNCHES NEW PARTS SHOP

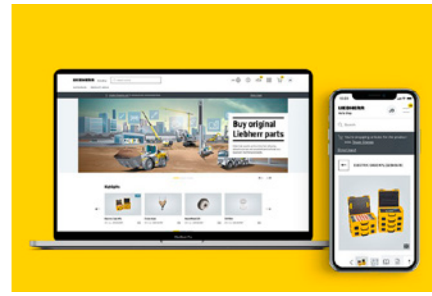

With the launch of the new Parts Shop, which will replace the ten existing shops, Liebherr is standardizing the extensive range of spare parts. From March 10, 2025, the Parts Shop is pooling together the entire range from all product segments, including earthmoving, material handling technology, deep foundation, maritime cranes, mobile and crawler cranes, tower cranes, concrete technology, gear technology, automation systems, mining and components, in one central location.

The new shop has been developed by Liebherr and so it is closely connected to the existing MyLiebherr services, such as the spare parts catalogue. As such, the Parts Shop can still be found via the MyLiebherr customer portal, though it can also be accessed directly too. MyLiebherr gives customers an extensive platform that provides access not only to spare parts, but also to important information about machines and services, as well as acting as a central point of contact for various Liebherr services.

With a modern and intuitive user interface together with improved performance, users of the new shop can expect a better user experience. The simple operation and fast response time enables customers to navigate their way around the products effortlessly and complete their orders efficiently. The check-out process will already be familiar to many customers. It is strongly orientated towards the Parts Order, an expert function introduced in the summer of 2024 that enables orders to be compiled and placed quickly. To find the items they need, customers can use the improved search function or browse the product areas or one of the spare part categories. All users can view the shop's product assortment. As before, to make a purchase in the shop, users must be registered and have an active business relationship with a Liebherr service partner.

liebherr.com

Index Corporation

ANNOUNCES REORGANIZATION AND TEAM ADDITIONS

Index Corporation has announced that Michael Huggett will succeed Cris Taylor as the company's president and CEO. Huggett will assume leadership of the company during a transition period in April 2025, concluding with Taylor's retirement at the end of that month.

Huggett brings with him over 30 years of industry experience. He started his career as a machinist, followed by roles of increasing responsibility at multiple prominent machine tool builders. Most recently, he has served as the director of sales for Index Corporation since early 2017.

"Over the past eight years, Index has significantly increased its annual sales in the North American market," says Reiner Hammerl, managing director–sales of Index Werke, the German parent company of Index Corporation. "Michael has played a vital role in that growth and in the transformation of our subsidiary. He possesses the perfect combination of experience and expertise to ensure that we continue to grow our customer base and evolve to meet their changing needs."

Taylor took the helm of Index Corporation in January 2021 and has overseen much of the company's growth. His retirement caps a 40-year career that began as a machine-building apprentice and culminated in serving as CEO of multiple machine tool organizations over the past two decades. In retirement, he plans to use his newfound free time to restore and work on his motorcycle collection and travel extensively.

Index has also announced a restructuring of its sales team that includes the addition of three new members and reorganization of its territories. Bryan Young has joined the company as national sales manager, while John Kemezis and Jason Shorette have joined as regional sales representatives.

index-group.com

KISSsoft

2025 AVAILABLE IN APRIL

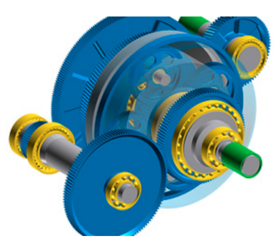

The new *KISSsoft Release* brings innovations and enhancements for results visualization, allowing you to design even more efficiently, precisely, and productively. Within Gleason's strategy "Design–Manufacturing–Measure," KISSsoft continues to add functions for simulating cylindrical gear manufacturing. After all, you target a gear design combining the highest strength with low manufacturing costs. KISSsoft offers a variety of rating procedures. Additionally, bearing ratings methods according to Timken have been added.

New functions include:

- Rollout—Root form diameter tolerance analysis
- Hobbing—Process time, interference check, hob shifting
- Timken catalog and adjusted bearing life
- Graphics and tables dashboards

kisssoft.com

United Grinding's

STOLMAR ELECTED TO AMT BOARD OF DIRECTORS

Markus Stolmar, president and CEO of United GrindingNorth America Inc., a subsidiary of the United Grinding Group, was recently elected to the Association for Manufacturing Technology (AMT) board of directors. AMT represents U.S.-based providers of manufacturing technology, speeding the pace of innovation, increasing global competitiveness and developing the industry's advanced workforce of tomorrow.

"I am both honored and filled with gratitude to join the AMT board, and I look forward to what's ahead," Stolmar said. "I am excited to collaborate with an exceptional group of industry leaders as we help to shape the future of U.S. manufacturing."

Stolmar joins newly elected AMT chairman of the board Michael Cicco, president and CEO of FANUC America Corp. Together, the AMT board will help U.S. manufacturers overcome competitive obstacles with innovative solutions that lead to opportunity and success.

grinding.com

MAY 12–15

Automate 2025

Between intimate workshops with industry giants, keynotes, networking events, innovation competitions and live demonstrations, Automate (Detroit) offers comprehensive automation education and cutting-edge robotics, vision, AI, motion control and other technologies. Keynote sessions highlight how these technologies solve real-world challenges while theater sessions cover important topics such as how robotics and automation are transforming the economy; innovative strategies for jumpstarting an automation strategy, or how companies can cultivate talents in the workforce. This year will again feature presentations from the finalists of the Automate Startup Competition.

geartechnology.com/events/automate-2025

MAY 13–14

CTI Symposium USA 2025

CO_2 reduction is critical for automotive drivetrain. Here the battery electric drive using renewable energy is the focus. What can we do to increase efficiency and reliability, reduce cost and at the same time reduce upstream CO_2? At CTI Symposium USA 2025 (Novi, MI) the automotive industry discusses the challenges it faces and promising strategies. The latest solutions in the fields of electric drives, power electronics, battery systems, e-machines as well as the manufacturing of these components and supply chain improvements are presented. In 2025, executives and experts of OEMs, suppliers and laboratories will discuss in various panels the actual challenges the industry is facing including how to manage the e-mobility transition 2.0, the impact of politics and consumer adoption.

geartechnology.com/events/cti-symposium-usa-2025

MAY 19–22

Cleanpower 2025

Cleanpower 2025 (Phoenix) grows businesses by gathering key decision makers and stakeholders across the wind, solar, storage, hydrogen, and transmission industries for discussion, deal making, networking and a whole lot of fun. The trade show not only brings together the different technologies that make up the renewables mix; onshore wind, offshore wind, solar, storage, and transmission but also the different segments within the industries; manufacturers, construction firms, owner operators, utilities, financial firms, corporate buyers and more. Cleanpower will feature the latest products, services and technologies coming to the renewable energy industry.

geartechnology.com/events/cleanpower-2025

JUNE 2–5

Reliable Plant 2025

This three-day event (Schaumburg, IL) offers attendees learning sessions and case studies on the latest industrial lubrication and oil analysis technologies. The comprehensive conference schedule covers every facet of the machinery lubrication industry and includes workshops on topics such as employee performance, lubrication fundamentals, condition-based maintenance and planning. Reliable Plant attendees come to the conference to connect with suppliers and service providers who can help them achieve bottom-line results in maintenance, reliability, and operations. From technicians and planners to management and leadership, you will be able to meet and influence entire buying teams at Reliable Plant. The event is co-located with Machinery Lubrication.

geartechnology.com/events/reliable-plant-2025

JUNE 15–18

PowderMet2025

PowderMet2025 (Phoenix) is dedicated to metal powder and particulate materials-based processes including press and sinter, metal additive manufacturing, metal injection molding and more. The show provides an energetic forum to showcase PM, metal AM, and MIM equipment, powders, products, and services. MPM2025, co-located with PowderMet 2025, is a technical conference and exhibition dedicated to metal additive manufacturing. Attendees can dive deep into the latest advancements in the field through insightful technical presentations and explore exhibits showcasing additive manufacturing technologies. Sessions include topics on material development, standards, metal density, and more.

geartechnology.com/events/powdermet-2025

AD INDEX

gear TECHNOLOGY®

FREE SUBSCRIPTION

24GTALL

☐ Renew my subscription ☐ NEW subscriber

☐ **YES** I want to receive/continue to receive ***Gear Technology*** ☐ **NO**

Name ____________________

Job Title ____________________

Company Name ____________________

Company Address ____________________

City ____________________

State ____________________

Zip Code ____________________

Signature: ____________________ *(required)*

Date: ____________

Please send

☐ PRINT Version

☐ DIGITAL Version (E-mail required)

E-MAIL: ____________________

☐ BOTH Print and Digital

*You can OPT OUT at any time.

How are you involved with Gears?

(Check all that apply)

☐ My company **MAKES** gears

☐ My company **BUYS** gears

☐ I **DESIGN** gears

☐ I am a **SUPPLIER** to the gear industry

☐ Other (please describe)

____

What is your company's principal product or service?

____

Your mailing label on the cover looks like this:

X/Y - means you have recieved a complimentary copy. Please complete this form to continue receiving your FREE copy of *Gear Technology*.

Q14 (shown above) - means you have 14 issues remaining in your subscription (a NEW subscription has 16 issues).

Q1 - means you have 1 remaining issue before your *Gear Technology* subscription expires. Please complete this form to renew.

MAIL to: 1001 N. Fairfax St, Suite 500, Alexandria, VA 22314 USA | SCAN to: *subscribe@geartechnology.com* | FAX to: 1.847.437.6618

ADDENDUM

A Tale of Two Timeframes

19th century steam engines to physical AI all in a two–week span

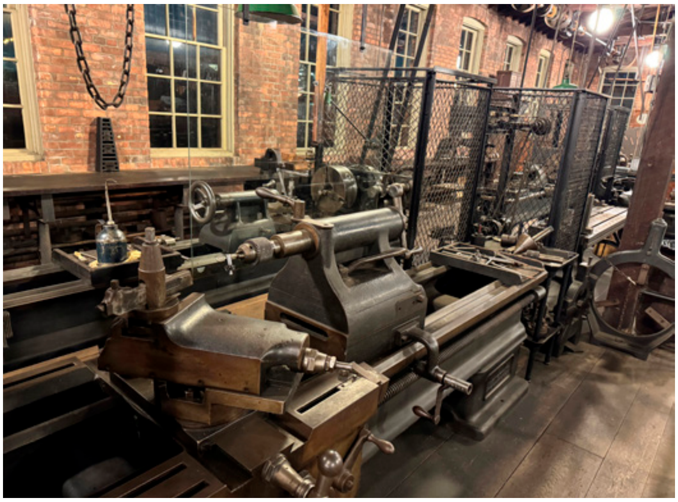

Matthew Jaster, Senior Editor

Two weeks separated my trips between the Armington & Sims Machine Shop and Foundry and my first venture to the Consumer Electronics Show (CES) 2025. The juxtaposition was noteworthy, particularly the sights, sounds and intentions of each trip.

Armington & Sims is part of Henry Ford's Greenfield Village in Dearborn, MI. The building boasts a system of shafts and pulleys distributing mechanical energy to rows of 19th-century machine tools. This is a replica of a multi-purpose job shop operating in Providence, RI, from 1889–1929.

Armington & Sims was a company known for producing an innovative line of stationary steam engines. By 1886, the Edison Illuminating Company had purchased more than 300 engines including those used in Thomas Edison's first commercial power plant in New York City.

Time traveling is part of Greenfield Village's endless charm. I walked through the shop and envisioned what it looked like in 1890—a full staff running the antique lathes, grinders and drill presses.

Two weeks later, I was in Las Vegas at CES 2025 where everybody wanted to talk about humanoid robots, AI and wearable technology. My two "field trips" were so diametrically opposed it was almost comical.

NVIDIA founder and CEO Jensen Huang kicked off CES 2025 with a 90-minute keynote that included new products to advance gaming, autonomous vehicles, robotics and agentic AI.

Huang introduced the NVIDIA *Cosmos* world foundation model platform, describing it as a game-changer for robotics and industrial AI. The next frontier of AI is physical AI, Huang explained. He likened this moment to the transformative impact of large language models on generative AI. "The ChatGPT moment for general robotics is just around the corner," he explained.

NVIDIA also announced *Mega* during CES 2025, an Omniverse Blueprint for developing, testing and optimizing physical AI and robot fleets at scale in a digital twin before deployment into real-world facilities. Imagine advanced warehouses and factories utilizing hundreds of autonomous mobile robots, robotic arm manipulators and humanoids working alongside people.

Mega offers enterprises a reference architecture of NVIDIA accelerated computing, *AI*, *Isaac* and *Omniverse* technologies to develop and test digital twins for testing AI-powered robot brains that drive robots, video analytics AI agents, equipment and more for handling enormous complexity and scale.

Project DIGITS represents NVIDIA's smallest yet most powerful AI supercomputer. "It runs the entire NVIDIA AI stack—all of NVIDIA software runs on this. DGX Cloud runs on this. Every software engineer, every engineer, every creative artist—everybody who uses computers today as a tool—will need an AI supercomputer," Huang said. Project DIGITS will launch in May.

On the CES show floor, I was also "starstruck" by how quick these technology advancements are coming. We're seeing lighter, smaller and more powerful components being produced for humanoid robots. Wearable AR devices—practical and compact—are showing up in business, healthcare and manufacturing. Dozens of software-defined vehicles are ready to challenge traditional automotive companies.

What will our shop floors look like 100 years from now? I may simply ask my AI-equipped smart glasses for a shop tour circa 2090, just to wrap my head around the possibilities.

For Related Articles Search
ai
at geartechnology.com

Gear Up for Large Gears

Choose the new 1200G Profile Grinding Machine for ultimate efficiency and flexibility in hard finishing of medium to large, high precision external and internal gears, or choose the 1200G Titan® with tool changer for highest precision and optional automation to produce large planetary gears and similar workpieces.
No matter which model you choose, benefit from revolutionary technology features like Wobble Compensation, Smart Dressing, different infeed strategies, and offer the highest precision on the market.

www.gleason.com/1200G

160 1865 2025

Total Gear Solutions Gleason